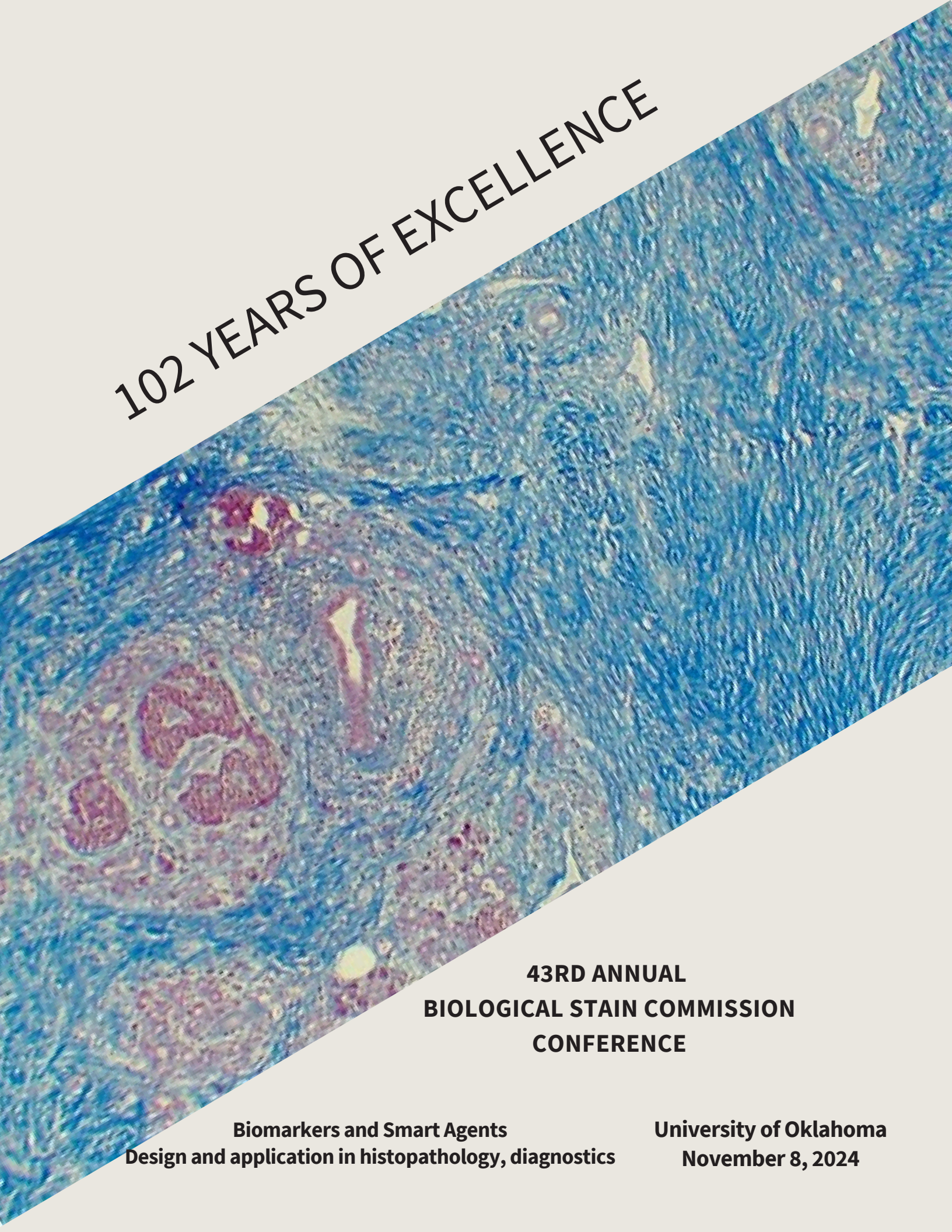

102 YEARS OF EXCELLENCE

43RD ANNUAL
BIOLOGICAL STAIN COMMISSION
CONFERENCE

Biomarkers and Smart Agents
Design and application in histopathology, diagnostics

University of Oklahoma
November 8, 2024

ABOUT THE BIOLOGICAL STAIN COMMISSION

The Biological Stain Commission (BSC) was established in 1923, and is recognized around the world as the standard quality control reference laboratory that certifies stains used in histology, biological, and research laboratories. The BSC Assay Laboratory is in the heart of the University of Rochester Medical Center, Rochester, NY, USA. The services provided as a non-biased party, directly support companies that sell histological stains. Histological stains that meet the quality standards of the BSC Assay Laboratory are endorsed as BSC Certified. This endorsement is often used by many as a quality control measure when buying stains for a laboratory.

The BSC strives to ensure the quality of dyes through independent testing according to appropriately rigorous chemical and performance criteria; promote cooperation and dialogue among manufacturers, vendors, and users of dyes for histochemical applications; educate users of biological stains about sources of reliable dyes and how they might best be used; and to publish information concerning new or improved uses for biological staining with dyes and related histochemical techniques in our peer-reviewed PubMed indexed journal, Biotechnic & Histochemistry, a journal of microtechnique and histochemistry.

Our annual meetings include a symposium with invited speakers, and strive to maintain active dialogue among scientists, engineers, manufacturers, and vendors concerned with staining techniques, techniques for imaging of stained tissue, and the application of staining in diagnostic medicine. There are also informal discussions and question and answer sessions on scientific and technical topics. We have hosted such annual meetings since 1980.

https://biologicalstaincommission.org/

WELCOME

Welcome to the 43rd Annual Biological Stain Commission Conference at the University of Oklahoma. The theme this year will be "Biomarkers and smart agents."

A biomarker is a characteristic that is measured as an indicator of normal biological or pathogenic processes, or as an indicator of responses to an exposure or intervention, including therapeutic interventions. Biomarkers can be evaluated through histology, radiography, and molecular or physiologic techniques.

Early histologists used various stains in tissue applications to study biologic and pathologic processes. Currently, other methodologies in tissue applications such as immunohistochemistry, radiographic imaging, molecular diagnostics, and fluorescence imaging are used to enhance or even replace the traditional staining process. All of these methodologies might be considered as potential biomarkers, depending on the setting they are used in.

Biomarkers that currently have clinical relevance include, but are not limited to: trichrome, reticulin, and PAS stains; immunohistochemistry for HER-2, ER, PR, Ki67, PD-L1, and PHH3; various in situ hybridization models; and, various DNA/RNA biomarkers. Other physiologic markers, tissue imaging techniques, and molecular markers are potential biomarkers that may have clinical relevance in the future.

In this 100th anniversary of the Biological Stain Commission, we discuss the past and current state of biomarkers in tissue application.

SCHEDULE AT-A-GLANCE

Time	Theme of Presentation	Speaker	Affiliation
8:00-9:00 a.m.	**Registration and Breakfast**		
9:00-9:30 a.m.	The Biological Stain Commission: An Introduction	Bruce Cochrane and Chad Fagan	Miami University Biological Stain Commission
9:30-10:00 a.m.	The Synthesis and Potential Biomedical Application of Cyanine and Cyanine Like Dyes: Donor Acceptor Fluorophores	Maged Henary	Georgia State University
10:00-10:25 a.m.	Targeted agents for identification of cancer	Lacey McNally	University Oklahoma Health Science Center
10:25-10:35 a.m.	**Break**		
10:35-11:00	Live-animal imaging to track invasive progression and extracellular vesicle signaling of ductal carcinoma in situ	Cole Hladik	University Oklahoma Health Science Center
11:00-11:30 a.m.	Immunohistochemistry Basics: Immunology to stained slide	Carol Bain	Indiana University
11:30-1:00 p.m.	**Lunch Break and Poster Presentations**		
1:00-1:30 p.m.	Utilization of immunohistochemistry in breast pathology	Mohamed Mokhtar Desouki	Roswell Park Comprehensive Cancer Center
1:30-2:00 p.m.	Structure-function relationships of small molecules biomaging probes from quantum chemistry modeling	Yihan Shao	University of Oklahoma
2:00-2:25 p.m.	Segment-based analysis of 18F-fluorothymidine positron emission tomography unveils significant prognosis predictor for hematopoietic stem cell transplantation therapy	Zheng Han	University of Central Oklahoma
2:25-2:35 p.m.	**Break**		
2:35-3:00 p.m.	Development of a novel pH low insertion peptide for imaging of pancreatic cancer using multispectral optoacoustic imaging	Ryan Bynum	University Oklahoma Health Science Center
3:00-3:30 p.m.	Troubleshooting immunohistochemistry	Sheila Criswell	University of Tennessee Health Science Center
3:30-4:00 p.m.	**Concluding Remarks and Poster Awards**		
4:00-5:00 p.m.	**BSC General Membership Meeting**		
5:30-7:30 p.m.	**Dinner** –Clark's Crew BBQ for registered attendees		

Immunohistochemistry basics: ihc basics: from immunology to a stained slide

Carol bain1*
1indiana university, department of pathology and laboratory medicine, histotechnology program
* cabain@iu.edu

Abstract
This presentation offers an overview of immunohistochemistry (ihc), guiding the audience from fundamental immunology to the staining of a tissue slide. The session begins with an introduction to basic immunological concepts, including the function of plasma cells in antibody production and the distinction between monoclonal and polyclonal antibodies. It then delves into how these antibodies are utilized to detect specific antigens within tissue samples, a cornerstone of ihc's specificity. Key steps of the ihc process, such as antigen retrieval, antibody application, and detection methods, will be explored in detail. The presentation will also cover various staining techniques, including chromogenic and fluorescent methods, which reveal antigen expression. In the final section, a practical walk-through of staining a tissue slide is provided, highlighting best practices. This presentation aims to equip the audience with a foundational understanding of ihc and its applications in research and diagnostics.

References
[1] dako. (2009). Education guide, immunohistochemical staining methods. Fifth edition
[2] suvarna, s. Kim, layton, c., & bancroft, j. D. (2019). Bancroft's theory and practice of histological techniques. Eighth edition. [oxford]: elsevier.
[3] donald van hecke (2002) routine immunohistochemical staining today: choices to make, challenges to take, journal of histotechnology, 25:1, 45-54

The Biological Stain Commission – An introduction

Bruce Cochrane1* and Chad Fagan2
1Professor Emeritus of Biology, Miami University (Ohio)
2Biological Stain Commission Assay Laboratory Manager
*[1] cochrabj@miamioh.edu
[2] Chad_Fagan@URMC.Rochester.edu

Abstract

The Biological Stain Commission was founded by Harold J. Conn and his associates in 1923 as a response to quality control issues stemming from the disruption in the supply of stains from Germany and the subsequent inconsistencies in domestically manufactured stains. From the beginning, the mission of the BSC included not only certification of histological stains, but also promoting cooperation among manufacturers, vendors and users of stains, public communication about them, and publication of scientific data1. One hundred years later, these objectives have been refined to include quality assurance, promotion of cooperation, education of users, and publication of new methods and applications. We will compare the challenges faced by the founders of the BSC with those we face today and discuss the opportunities the BSC has to strengthen and expand its mission.

References

[1] D. P. Penney,Biotechnic and Histochemistry 75 (1975) 154-166.

Troubleshooting Immunohistochemistry

Sheila Criswell1*
1University of Tennessee Health Science Center, College of Health Professions, Department of Diagnostic and Health Sciences
* scriswel@uthsc.edu

Abstract
One of the most exciting areas to work in the histology laboratory is the immunohistochemistry (IHC) department. Although numerous automated platforms exist to increase productivity and reproducibility, they are not without challenges, and some laboratories rely on manual methods for IHC which require a higher level of understanding for the process. IHC is a critical technique which enables the visualization of specific antigens in tissue sections. However, achieving optimal labeling can be challenging due to various technical issues. This presentation outlines common problems encountered in IHC and provides strategies for troubleshooting. Key issues include non-specific labeling/high background, weak signals, or lack of labeling in positive control tissues. Non-specific staining often arises from inadequate blocking, antibody cross-reactivity, or extended incubation times among other causes. Weak or absent signals may result from insufficient antigen retrieval or low antibody affinity, necessitating adjustments in retrieval methods and antibody concentrations. Problems may also arise from improper tissue preparation or excessive antibody concentrations. The importance of using appropriate positive and negative controls is emphasized to validate the specificity and sensitivity of the staining. By systematically addressing these issues, researchers can enhance the reliability and reproducibility of IHC results, thereby advancing the understanding of tissue-specific protein expression and its implications in health and disease.

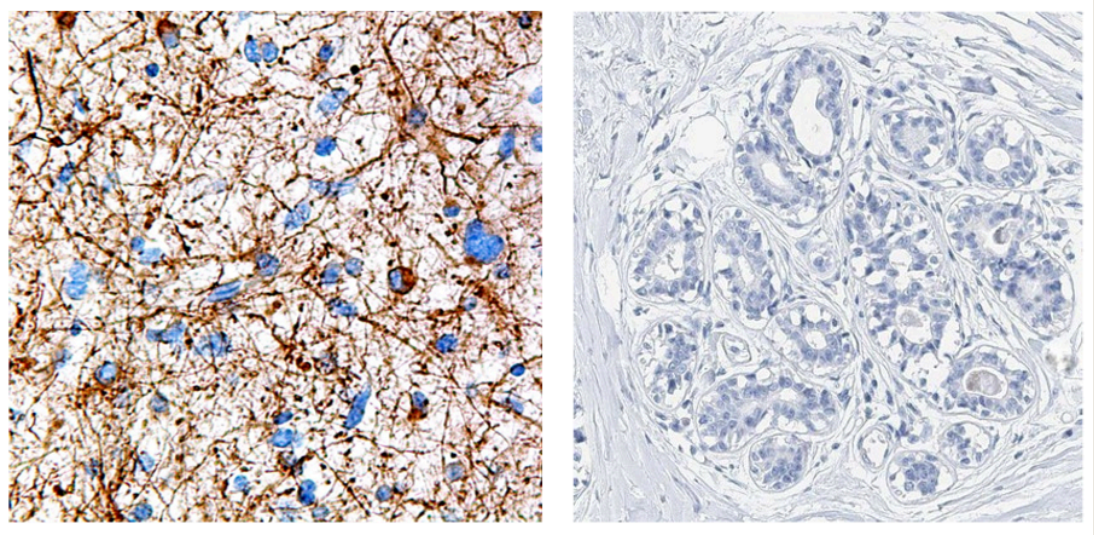

Figure 1. Example of control tissue (a) labelling with brown chromogen using immunohistochemistry, and patient tissue (b) lacking the chromogen. Reasons for discrepant labelling are manifold and may represent normal findings or problems with the immunohistochemistry technique.

References
[1] Sigma Millipore: Tips and Techniques for Troubleshooting Immunohistochemistry (IHC) https://www.sigmaaldrich.com/US/en/technical-documents/protocol/protein-biology/immunohistochemistry/antibody-immunohistochemistry-expert-tips-and-techniques#staining
[2] Thermo Fisher Scientific: IHC Troubleshooting Guide. https://www.thermofisher.com/us/en/home/life-science/protein-biology/protein-biology-learning-center/protein-biology-resource-library/pierce-protein-methods/ihc-troubleshooting-guide.html
[3] Cell Signaling Technology: Immunohistochemistry (IHC) Troubleshooting Guide & the Importance of Using Controls. https://www.cellsignal.com/learn-and-support/troubleshooting/ihc-troubleshooting-guide

Segment-based Analysis of 18F-fluorothymidine Positron Emission Tomography Unveils Significant Prognosis Predictor for Hematopoietic Stem Cell Transplantation Therapy

Zheng Han1*, Lacey McNally2, Jennifer Holter-Chakrabarty2
1University of Central Oklahoma
2 University of Oklahoma Health Sciences Center
* zhan1@uco.edu

Background: Clinical outcomes of hematopoietic stem cell transplantation (HSCT) following host hematopoiesis irradiation are variable, and early prediction of transplantation outcomes is crucial to manage relapses effectively. 18F-fluorothymidine (18F-FLT) positron emission tomography (PET) is promising in this regard, yet manual segmentation and analysis of different bone segments in 18F-FLT PET images is time-consuming and hinders its clinical adoption.
Methods: This study explores the use of a deep neural network (3D U-Net) to facilitate segment-based analysis (Fig.1A), aiming to identify predictive imaging features for relapses post-HSCT. A retrospective study included 22 patients (18–50 years) who received 18F-FLT PET scans within 12 h before (d0), 5-12 days after (d5-12), and 28 days after irradiation (d28), with follow-up for up to one year to monitor relapses. The dataset contains 45 CT volumes and ten manually segmented CT volumes were used to train the 3D U-Net, which was tested on the remaining 35 volumes. A random-forest model was employed to analyze 18F-FLT uptake data and identify segments with high predictive value of relapsing events based on feature importance score using the inherent explainer of scikit-learn. A threshold by which to predict relapsing events based on segments was found using Youden Index.

Results: The 3D-U-Net allowed accurate segmentation of bones based on CT volumes (Fig. 1B&C), with a high accuracy illustrated by the confusion matrix (Fig.1D) and an average dice score of 0.965 in the testing dataset. Segment-based analysis clearly identified differences in 18F-FLT uptake between relapsing and non-relapsing patients at d0 and d5-12 in different segments, particularly in thoracic and lumbar/sacrum regions. Notable higher intensities at d0 in relapsing patients compared to non-relapsing patients were observed The random-forest model identified 18F-FLT uptake in thoracic segment at d0 as a significant predictor of relapse (Fig.1E), which was consistent with the observation of remnant 18F-FLT signal at thoracic region in images (Fig.1F). To facilitate clinical adoption, a threshold of 0.14% ID/g of the thoracic region at d0 was developed, which was shown to effectively distinguish relapsing from non-relapsing patients in our cohort ($p<0.0053$). In contrast, pelvis region, which conventionally was thought of as an important predictor, did not show significant predictive value (Fig.1G).

Conclusions: This study demonstrates the clinical utility of 3D segmentation by deep neural networks for monitoring HSCT patients, revealing thoracic region at d0 as a critical imaging feature predictive of relapse.

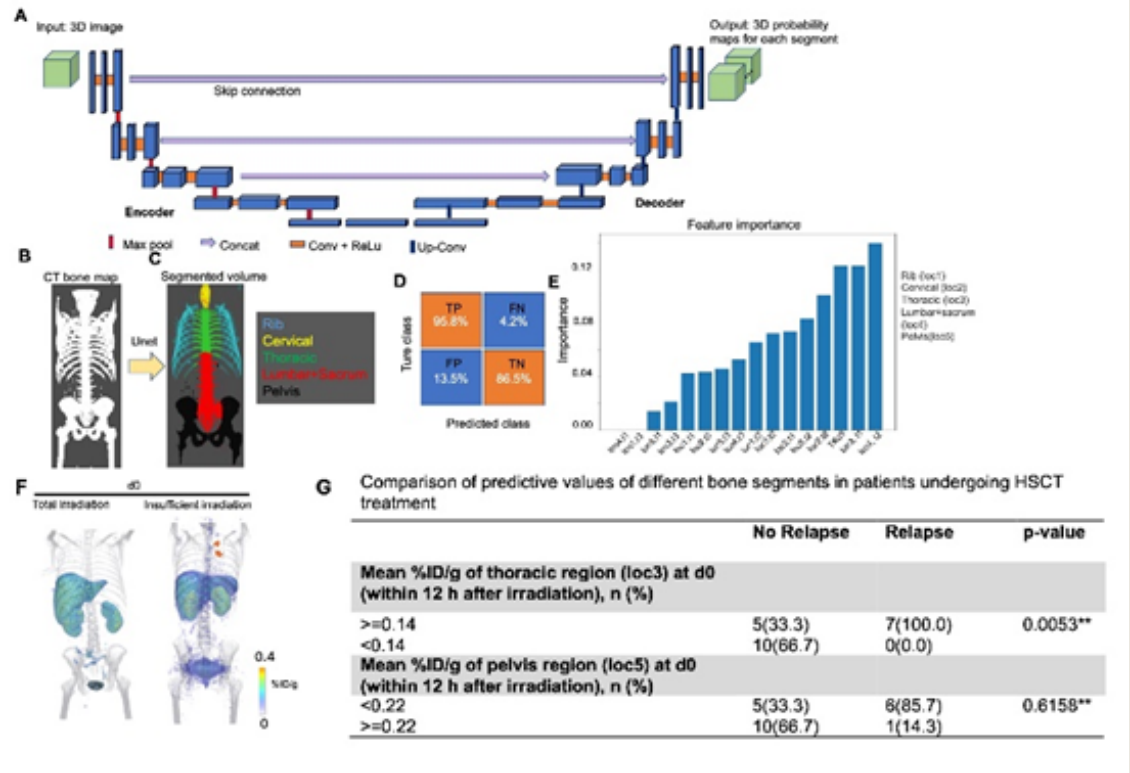

G Comparison of predictive values of different bone segments in patients undergoing HSCT treatment

	No Relapse	Relapse	p-value
Mean %ID/g of thoracic region (loc3) at d0 (within 12 h after irradiation), n (%)			
>=0.14	5(33.3)	7(100.0)	0.0053**
<0.14	10(66.7)	0(0.0)	
Mean %ID/g of pelvis region (loc5) at d0 (within 12 h after irradiation), n (%)			
<0.22	5(33.3)	6(85.7)	0.6158**
>=0.22	10(66.7)	1(14.3)	

Fig.1. A. Illustration of the architecture of 3D-Unet architecture, which consists of a four-layer encoder and a four-layer decoder, which contracts and expands dimensions of 3D CT volumes in a step-wise manner. (B, C) An exemplary image showing color-coded segmented volume (C) based on the corresponding CT bone map (B). D. A confusion matrix showing high prediction performance of the trained Unet. E. Feature importance values of different segments in determining relapsing risk as unveiled after training a random forest model. F. Representative 3D rendering of whole-body PET volumes (jet color) co-registered with CT volumes (gray) within 12 after irradiation. A patient showing total bone marrow irradiation (left) and another patient with insufficient irradiation (right) are shown. Arrow: remnant 18F-FLT uptake in thoracic region. G. Value of segment-based analysis of thoracic region and pelvis region in predicting relapses at d0 (within 12 h after irradiation).

The Synthesis and Potential Biomedical Applications of Cyanine and Cyanine Like Dyes “Donor Acceptor NIR Fluorophores”

Maged Henary*1,2,, Guliz Ersoy Ozmen1, Ranju Ghimiere1, Zaryab Gul1, Diana Alcaraz1 and Hak Soo Choi3

1Department of Chemistry, 2The Center for Diagnostics and Therapeutics, Georgia State University, 100 Piedmont Road SE, Atlanta GA, 30303 USA. 3Gordon Center for Medical Imaging, Division of Nuclear Medicine and Molecular Imaging, Department of Radiology, Massachusetts General Hospital and Harvard Medical School, Boston, Massachusetts 02114, USA.

Abstract:

NIR fluorescent compounds offer two major advantages over small molecules, which emit at visible wavelengths. First, biological tissues have lower absorption of NIR light, this enables NIR light to penetrate deeper into tissue than the compounds emit light at visible wavelengths, thus enabling the assessment of data from deeper structures. Second, less autofluorescence is present at the NIR compared to visible wavelengths, enabling higher signal-to-background ratios. Therefore, molecular probes that emit light within the NIR region are expected to be suitable for bioimaging and tumor targeting. Cyanine dyes are one of NIR fluorophores, which consist primarily of two terminal heterocyclic rings containing nitrogen connected by a polymethine chain. These heterocyclic rings serve as electron donors and acceptors, which results in the delocalization of electrons across the polymethine chain, allowing a longer wavelength of absorption to be observed. Cyanine dyes can also be categorized into mono-, tri-, penta- and heptamethine compounds according to the number of methine chains between the two terminal heterocyclic rings.

Recently we discovered a new class of cyanine like donor-acceptor fluorophores, which absorbs and fluoresces in the NIR. Donor acceptor fluorophores consist of three units as donor, acceptor and linker, introduce a push pull system that can have superior impact on the structure properties. In my talk, we demonstrate our work in the field of cyanine dyes as well as the synthesis and potential applications of donor-acceptor fluorophores

Structure-Function Relationship of Small-Molecule Bioimaging Probes from Quantum Chemistry Modelling

Yihan Shao1,*, Carly Wickizer,1 Vardhan Satalkar,2 Chongzhao Ran,3 Lacey McNally4
1Department of Chemistry and Biochemistry, University of Oklahoma, Norman, OK 73019
2Southeast Center for Mathematics and Biology, Georgia Institute of Technology, Atlanta, GA 30332
3Athinoula A. Martinos Center for Biomedical Imaging, Department of Radiology, Massachusetts General Hospital/Harvard Medical School, Boston, MA 02119
4Stephenson Cancer Center, University of Oklahoma, Oklahoma City, OK 73104
* yihan.shao@ou.edu

Abstract
In the development of small-molecule fluorescent, bioluminescent, chemiluminescent, and optoacoustic imaging probes, it is essential to understand how structural changes to a dye molecule affect its absorption/emission wavelengths, absorption strength, and fluorescence quantum yields. In the last several years, we employed quantum chemistry calculations to explore these structure-property relationships. In this presentatation, we report our findings for oxyluciferin (firefly bioluminescence) [1], ADLumin (chemiluminescence) [2,3], and Squaraine (optoacoutstic imaging) [4].

References
[1] Vardhan Satalkar, Enrico Benassi,* Yuezhi Mao,* Xiaoliang Pan, Chongzhao Ran, Xiaoyuan Chen, and Yihan Shao,* "Computational Investigation of Substituent Effects on the Fluorescence Wavelengths of Oxyluciferin Analog", Journal of Photochemistry and Photobiology A, 431 (2022) 114018.
[2] Jing Yang, Wei Yin, Richard Van, Keyi Yin, Peng Wang, Chao Zheng, Biyue Zhu, Kathleen Ran, Can Zhang, Mohanraja Kumar, Yihan Shao, and Chongzhao Ran,* "Turn-on chemiluminescence probes and dualamplification of signal for detection of amyloid beta species in vivo," Nature Communications 11 (2020) 4052.
[3] Jing Zhang, Carly Wickizer, Weihua Ding, Richard Van, Liuyue Yang, Biyue Zhu, Jun Yang, Can Martin Zhang, Shiqian Shen, Yihan Shao, and Chongzhao Ran,* "In Vivo Three-dimensional Brain Imaging with Chemiluminescence Probes in Alzheimers Disease Models", Proceedings of National Academy of Sciences, 120 (2023) e2310131120.
[4] William M. MacCuaig,Carly Wickizer, Richard S. Van, Megan R. Lerner, William E. Grizzle, Yihan Shao, Maged Henary,* and Lacey R. McNally,* "Influence of structural moieties in squaraine dyes on optoacoustic signal shape and intensity", Chem, 10 (2024) 713.

Acknowledgements
The authors wish to thank the National Institutes of Health for financial support through grants R01GM135392, R35GM153297 (YS), R21AG059134, R01AG055413 (CR), and F31CA261044, R01CA205941, R01EB034731, R01CA281098, P30CA225520 (LM).

Targeted agents for identification of cancer

Lacey McNally, Ryan Bynum, Happy Agarwal, Karl Thomas

University of Oklahoma Health Science Center

Optoacoustic imaging is based upon an approach where absorbed electromagnetic energy (e.g., NIR light) results in a thermoelastic expansion which converts into detectable ultrasonic waves. Real-time, high spatial-resolution, and volumetric imaging is possible because of the selective absorption of light at multiple wavelengths which distinguish both endogenous and exogenous contrast agents. Traditionally, exogenous contrast agents detected using optoacoustic imaging have largely exploited commercially available near-infrared dyes, including IR-800-CW, IR-780, indocyanine green (ICG), and methylene blue, or nanoparticles, particularly iron oxide particles or gold nanorods. We have developed both disease specific peptide-based contrast agents for the detection of cancer as well as identified substituents of small molecule dyes which result in increases in optoacoustic signals. Both the peptide-based contrast agents and small molecule dyes were assessed in vivo using optoacoustic imaging.

Prevalence of Helicobacter pylori in routine adult tonsillectomies

Leica Barnhart BS1, Chloe Balzer BS1, and Sheila Criswell PhD1
1 Department of Diagnostic and Health Sciences, University of Tennessee Health Science Center, Memphis, TN, USA

Helicobacter pylori, a curved bacterial rod and causative agent of peptic ulcer and gastric adenocarcinoma, is found as an infectious agent in the stomach of over half of the global population. H. pylori has been identified in oral biofilms and its presence in adenotonsillar tissues has been suggested, with variations in testing methodology both proving and disproving its presence. The current study employed 119 formalin-fixed paraffin-embedded tonsillar tissues from an adult population (n=86) in a major metropolitan city with immunohistochemistry procedures using a monoclonal antibody to determine the incidence of H. pylori in the tonsils. H. pylori was identified in 72.1% of the patients and was associated with Actinomyces spp. in 92.0% of those cases. The high incidence of H. pylori in patients undergoing tonsillectomy suggests that H. pylori may be a contributing factor for tonsillitis and tonsillar hypertrophy. Furthermore, the reservoir for H. pylori in the tonsils may explain why some persons remain refractory to antibiotic treatment for gastric H. pylori.

Table 1. Patient and sample positivity for *Actinomyces spp*. and *H. pylori* in tonsil tissues.

	Actinomyces (+) patients / tonsils	*Actinomyces* (-) patients / tonsils
H. pylori (+)	57 (66.3%) / 70 (58.8%)	5 (5.8%) / 6 (5.0%)
H. pylori (-)	14 (16.3%) / 17 (14.3%)	10 (11.6%) / 26 (21.8%)
	Total of 86 patients and 119 tonsils	

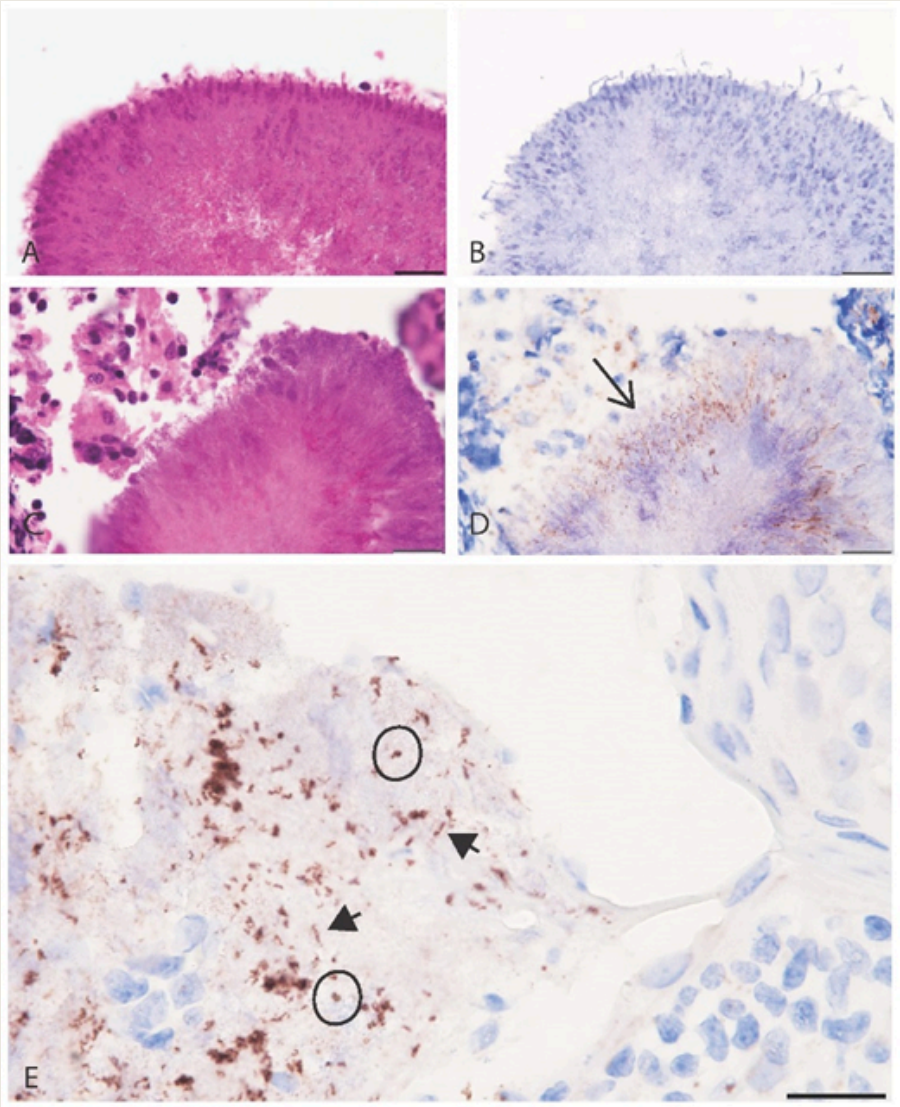

Figure 1. Actinomyces and H. pylori in tonsils. Actinomyces stained with H&E (A, C) exhibits a characteristic filamentous radial growth pattern which may be better visualized with immunohistochemistry hematoxylin counterstain (B, D) taken from serial sections of (A, C). Section (B) is negative for H. pylori labeling, but section (D) demonstrates H. pylori bacteria (black arrow) which cannot be readily visualized with H&E (C). H. pylori (E) were identified most frequently in their coccoid form (circled), but in a few sections, they appeared as curved or spiraled rods (arrow heads). Scale bars = 20 µm.

ENDOMETRIAL CANCER PREVENTION THROUGH SHetA2: AN INNOVATIVE CONSERVATIVE STRATEGY

Rajani Rai, Debasish Kumar Dey, Vishal Chandra
Gynecologic Oncology Section, Obstetrics and Gynecology Department, Stephenson Cancer Center, University of Oklahoma Health Sciences Center, Oklahoma City, OK 73104, USA.

Abstract
The incidence and mortality rates of endometrial cancer (EC) are on an upward trajectory. The clinical effectiveness of current standard treatments such as total hysterectomy and hormonal therapy is limited in obese and younger patients due to surgical complications, loss of fertility and weight gain. Endometrial intraepithelial neoplasia (EIN) is a precursor of EC and the reversal of EIN to normal endometrial histology presents a promising avenue for preventing the development of EC. Previously, our investigations revealed the anticancer properties of SHetA2, a novel, small, and non-toxic drug, against EC. Building on these prior findings, we postulated that SHetA2 could inhibit endometrial cell proliferation through cyclin D1 degradation and impede ERα mitochondrial translocation by disrupting the colocalization of estrogen receptor/ERα and Grp75.
In our study, SHetA2 was administered orally and locally in the uterus via a polymer rod in an estrogen-induced EIN rat model established in our laboratory. The development of estrogen-induced EIN was confirmed by the notably higher uterine weight, increased endometrial and glandular areas, and upregulation of proliferative markers in estrogen-supplemented animals. SHetA2 treatment significantly reversed these effects, with greater regression observed in animals receiving localized rather than oral delivery of SHetA2. Pharmacokinetic analysis by high-performance liquid chromatography (HPLC) revealed higher SHetA2 concentrations in the liver following oral administration compared to local delivery.
Mechanistically, SHetA2 treatment minimized ERα-Grp75 colocalization as evidenced by immunofluorescence imaging. Immunoblotting confirmed decreased expression of cyclin D1 and PCNA. Enzyme-linked immunosorbent assay (ELISA) confirmed the reduced activity of manganese superoxide dismutase (MnSOD) in the estrogen-induced EIN model. In summary, suppression of ERα-GRP75 colocalization and cyclin D1 levels by SHetA2 supports our hypothesis. Overall, our findings underscore SHetA2's potential to suppress estrogen-induced EIN development. The localized delivery system-maintained drug efficacy in the target tissue while minimizing off-target absorption. These results warrant further exploration for SHetA2 polymer rods as intrauterine devices.

Acknowledgment: This work was supported by the "IDeA Network of Biomedical Research Excellence (INBRE) grant".

Histological Methods for Plants

Sheila Criswell1, Brian Gaylord2, Christopher R. Pitzer3

1 Department of Diagnostic and Health Sciences, University of Tennessee Health Science Center, Memphis, TN, USA
2 UT DermPath, a division of University Clinical Health, University of Tennessee Health Science Center, Memphis, TN, USA
3 Department of Physiology, College of Graduate Health Sciences, University of Tennessee Health Science Center, Memphis, TN, USA

The authors explored the histological challenges of working with plant tissues by collecting various flora representing the four main plant organs: leaf, stem, root, and flower/fruit. Triplicate samples of each specimen were placed in formalin for paraffin embedding, in formalin for later frozen sections, and used fresh for immediate frozen sectioning. Frozen sections of plant tissues were more challenging to obtain than formalin-fixed paraffin-embedded (FFPE) sections, showed tissue loss during staining, and were morphologically inferior to FFPE sections. Historically, plant tissue fixation and processing have used different reagents compared to animal tissue processing and required significantly longer times. However, this investigation found that reagents and protocols from a modern histology laboratory processing mammalian tissues can be applied to plant tissue processing with only slight modifications in reagent timing. Additionally, while it is well-known that plant cell walls stain well with safranin O, this study found that the uptake of safranin O can be accelerated by incubating at 60°C.

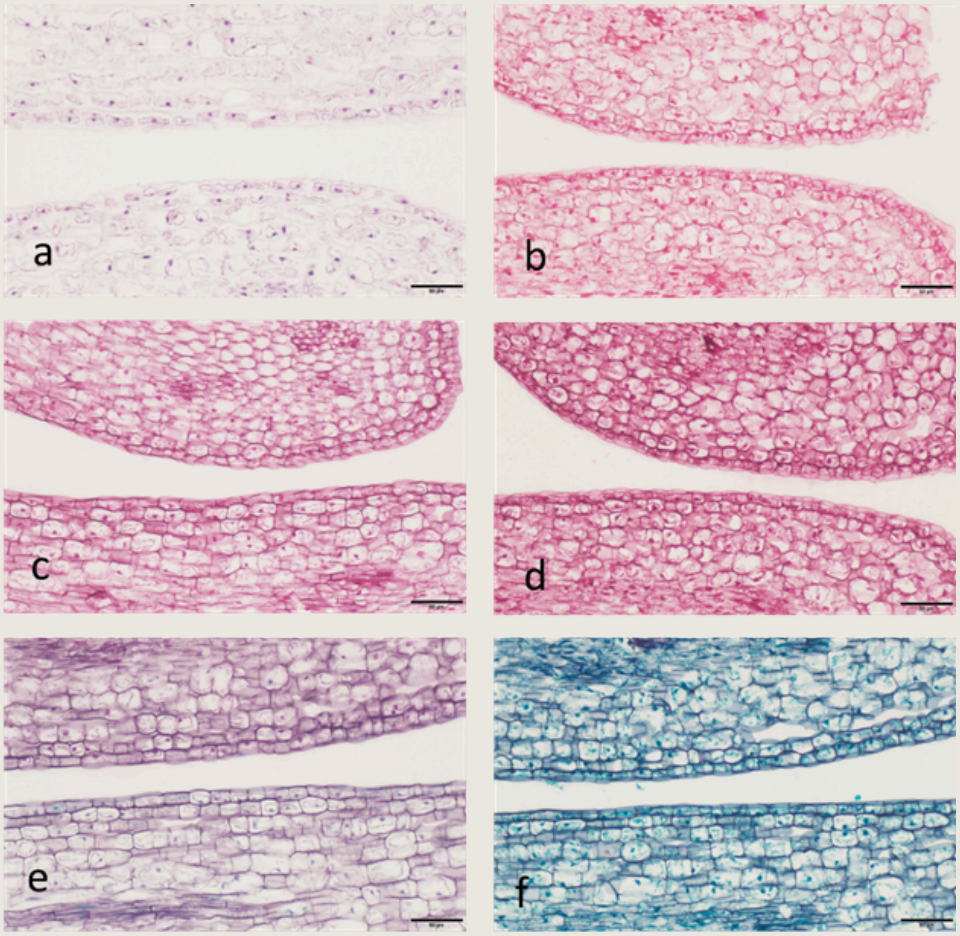

Figure 1. Formalin-fixed paraffin-embedded sections of broccoli stained with (a) H&E which shows good nuclear staining, but poor cytoplasmic staining. However, tissues stained with Safranin O for (b) 1 hour at room temperature demonstrates improved cytoplasmic staining. Safranin O stain at (c) room temperature for 24 hours or at (d) 60°C for 1 hour show similar improved staining over (b). The fast green counterstain (e,f) applied for 1 minute after safranin O appeared less vibrant when dehydrated through alcohols (e) when compared to the air-dried method of dehydration (f). Scale bar = 50 µm.

The Impact of Gliomas on the Normal Brain Microenvironment: A Pilot Study

Nicole L. Riha, Jacen S. Moore, Sheila Criswell
College of Health Professions, University of Tennessee Health Science Center, 930 Madison Ave., Memphis, TN

Gliomas are malignant tumors of neuronal support cells within the central nervous system (CNS) and are characterized by poor overall prognoses and limited treatment options due to their infiltrative growth patterns. The neural tumor microenvironment, composed of benign neurons, neuroglia, endothelial cells, and intravascular white blood cells, is a target-rich site for potential chemotherapeutic agents. This study assessed cell proliferation rates, white blood cell components, and a limited number of nuclear, cytoplasmic, and membrane markers using immunohistochemistry (IHC) assays on formalin-fixed and paraffin-embedded benign and glial tumor tissue samples from the CNS. It was observed that glioma tissues had increased rates of glial cell proliferation, and significant increases in the number of observed T-lymphocytes and granulocytes, but decreased expression of markers SSTR2, L1CAM, and GATA3 when compared to benign tissue samples. A more detailed characterization of the migratory and population expansion potential of the gliomal microenvironment could provide valuable therapeutic target combinations for use in the development of future treatments.

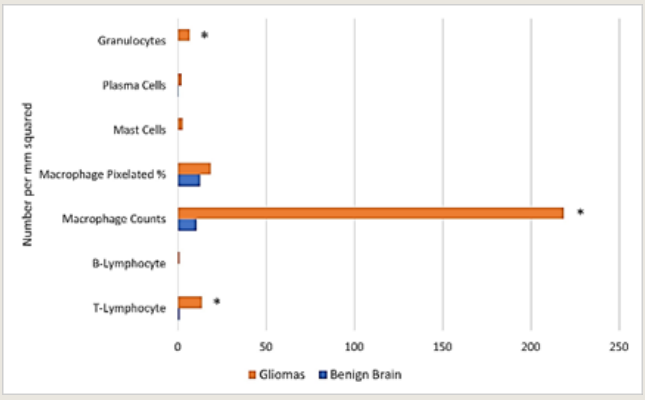

Figure 1. Figure 3. Immunohistochemistry labeling results for white blood cell populations between gliomas and normal brain tissues. Granulocytes and T-lymphocytes were found to be statistically increased in glioma tissues. Although macrophages were noted to be increased in gliomas in both methods of enumeration, they did not reach statistical significance for the automated method to determine percent labeling in tissues.

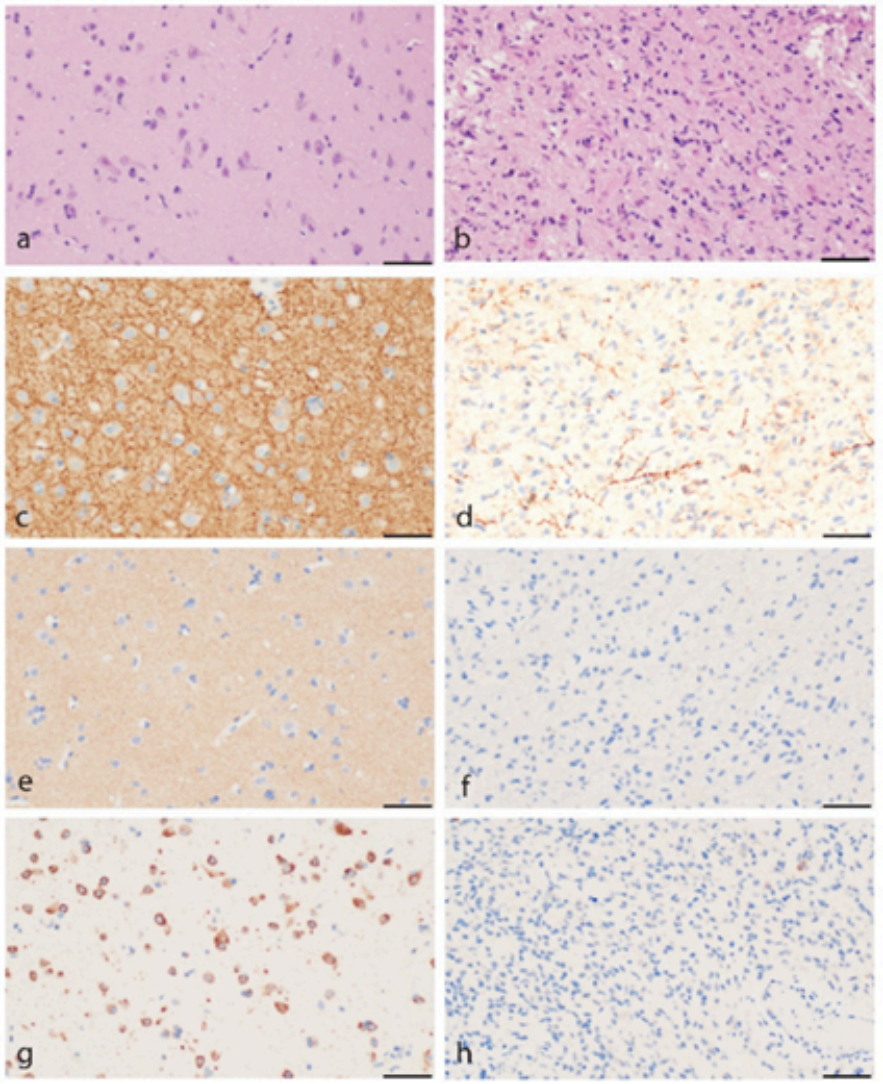

Figure 2. Benign CNS and glioma tissues with H&E and labeled with diaminobenzidine immunohistochemistry. (a) Benign and (b) malignant CNS stained with H&E. (c) Positive labeling (brown chromogen) of SSTR2 in benign brain tissues as compared with (d) glioma which evidenced a lower receptor expression. (e) Increased L1CAM expression in benign tissue as compared with (f) gliomas. (g) Higher GATA3 transcription factor expression in benign tissues as compared with (h) gliomas. Scale bar = 50 µm. Images were taken with 40x objective.

Christina Henson, MD, Ahmad K. Abou-Foul, MD, Christine Glastonbury, MBBS, Shao Hui Huang, MD, Professor Ann D. King, FRCR, William M. Lydiatt, MD, Lachlan McDowell, MBBS, Alex A. Nagelschneider, MD, Paul C Nankivell, PhD, Professor Brian O'Sullivan, MD, Rhian Rhys, FRCR, Youping Xiao, MD, Eugene Yu, MD, Professor Sue S Yom, PhD, Professor Hisham Mehanna, PhD

Criteria for the diagnosis of extranodal extension detected on radiological imaging in head and neck cancer: HNCIG international consensus recommendations

Purpose/Objectives Pathological evidence of extranodal extension (pENE) is known to be a negative prognostic factor in head and neck cancer (HNC). The available evidence suggests that radiologically or imaging-detected extranodal extension (iENE) is also associated with worse clinical outcomes. Although the reliable detection of iENE before initiation of treatment may help guide treatment selection, the diagnostic criteria and terminology used to report iENE are not widely agreed upon. The Head and Neck Cancer International Group (HNCIG) conducted a Delphi survey with the aim of developing a framework for decision-making on the most important areas of iENE diagnostic criteria and terminology requiring consensus.

Materials/Methods All 21 international member groups of the HNCIG were invited to nominate a practicing radiologist with HNC expertise to join the global consensus panel. A three-round modified Delphi process with 18 international radiology experts representing 14 national clinical research groups was completed. Online questionnaires via the Qualtrics platform included four main sections pertaining to iENE: diagnostic criteria, inter-observer agreement, the impact of core biopsy, and classification systems.

Results [LM1] [SHH2] We generated consensus recommendations on the terminology and criteria for iENE to harmonize clinical practice and research. Overall, we achieved consensus on 47 items. The experts strongly agreed that there is no difference in iENE features between HPV-positive and HPV-negative HNC. Regarding iENE features, the experts strongly agreed that indistinct nodal margin, extension into perinodal fat, extension into adjacent structures, and conglomerate/matted/coalescent nodes should all be used as criteria by which to identify iENE, while nodal necrosis and capsular thickening should not be used as criteria for identifying iENE. The experts also agreed that “conglomerate”, “matted”, and “coalescent” do not describe different things. Importantly, we also proposed a new 5-tier classification system to aid diagnosis, which was supported by the majority of respondents over existing systems but which will require clinical validation. The experts strongly agreed in support of using a standardized classification system and synoptic reporting for iENE. The recommendations have been endorsed by 19 national organisations, representing 34 countries.

Conclusion These guidelines will serve to standardize definitions and classifications to aid reporting in both clinical practice and research. We have also proposed a new classification system for the diagnosis of iENE that requires validation before wider clinical implementation.

Establishing and Evaluating a Mouse Model For Cancer Cachexia

Jingxuan Yang,1* Zhijun Zhou,1 Arreola Arreola,1 Yang Cai,1 Yuqing. Zhang,1 Courtney Houchen,1 Min Li,1

1Department of Medicine and 2Department of Surgery, The University of Oklahoma Health Sciences Center, Oklahoma City, OK.

* Jingxuan-Yang@ouhsc.edu

Introduction: Most pancreatic cancer (PC) patients develop cancer cachexia syndrome, characterized by uncontrollable body weight loss, lack of appetite, muscle wasting, and adipose loss. This syndrome is associated with nearly 80% of deaths in advanced PC. There is a pressing need to identify potential therapeutic targets and develop effective treatment options for cancer cachexia.

Methods: Mouse models are critical for studying cancer cachexia, a systemic disorder involving various organs that cannot be recapitulated by in vitro models. Through orthotopic implantation of human/murine PC cells in nude mice or C57BL/6 mice for xenograft / allograft tumors, we established a cancer cachexia mouse model.

Results: Here, we describe a protocol for the establishment of cancer cachexia mouse models and the evaluation of cancer cachexia. We detail the steps in preparing tumor cells for inoculation and surgical procedures. After establishing these mouse models, we include the methods for monitoring cancer cachexia, including grip strength evaluation, tissue collection, and calculation of cross-sectional areas of muscle tissue.

Conclusion: We present a step-by-step procedure for establishing a cancer cachexia mouse model and methods to evaluate cancer cachexia, including muscle wasting and adipose loss.

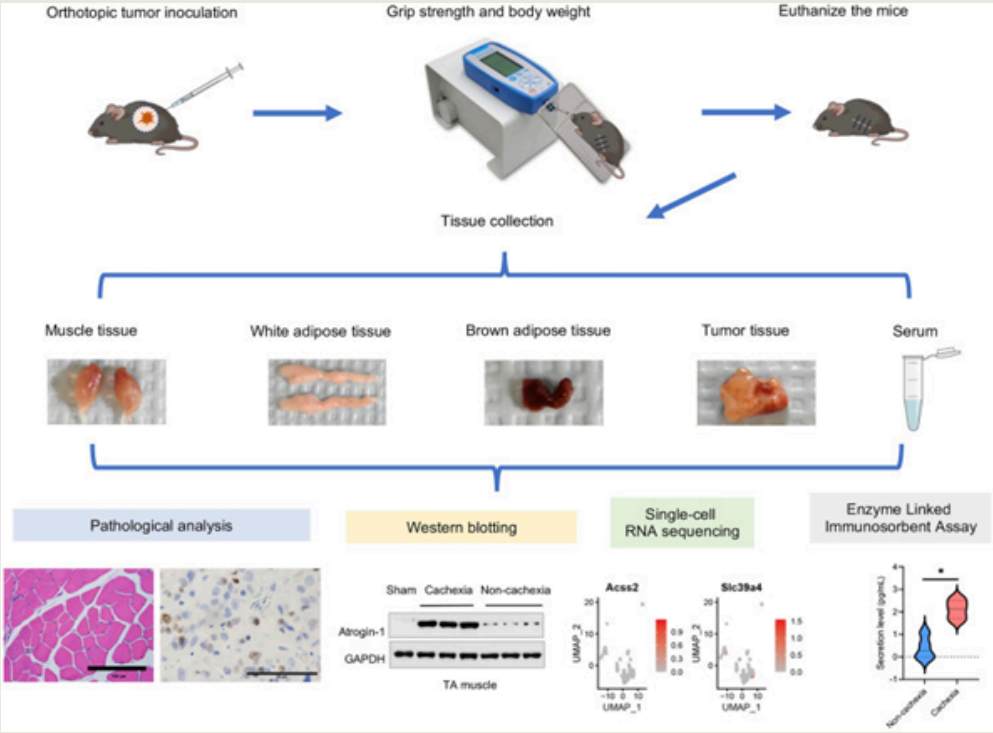

Figure 1. Establishment of cancer cachexia mouse model and tissue collection for subsequent analyses

References

1. Liu, M., Ren, Y., Zhou, Z., Yang, J., Shi, X., Cai, Y., Arreola, A.X., Luo, W., Fung, K.M., Xu, C., et al. (2024). Cancer Cell 42, 885–903.e4.

2.Yang, J., Zhang, Z., Zhang, Y., Ni, X., Zhang, G., Cui, X., Liu, M., Xu, C., Zhang, Q., Zhu, H., et al. (2019). Gastroenterology 156, 722–734.e6.

POST DOC

Enhancing the dynamic range of Syndecan-1 peptide for targeted imaging of IGFR overexpressing pancreatic tumor using MSOT

Happy Agarwal, PhD, Ryan Bynum, Lacey R. McNally, PhD

1 Happy Agarwal, Postdoctoral Fellow, Stephenson cancer center, OUHSC, USA
* Lacey-Mcnally@ouhsc.edu

Abstract

Objective: Inaccurate determination of resection margin during surgery coupled with insufficient early diagnosis of pancreatic ductal adenocarcinoma (PDAC) represents major challenges in the treatment of the disease. Conventional imaging modalities such as ultrasound and near-infrared fluorescent imaging (NIR) are limited by poor spatial resolution, low imaging fidelity, light attenuation challenges at tissue depth for orthoptic models. This work is focussed on improving the dynamic range of syndecan-1 peptide (SDC1) for enahnced detection of IGFR overexpressing PDAC tumor1, 2. MSOT is used as a primary imaging modality to access the tumor specificty of our self designed SDC1.H probe with high sensitivity in an orthotopic murine model.

Methods: SDC1.H peptide were synthesized using the microwave chemistry (>90% purity). SDC1.H peptide was conjugated to HiLyte Fluor 750 dye to obtain NIR fluorescent probe for targeted imaging of PDAC. The peptide-dye conjugation was confirmed with UV-Vis spectroscoipy and the tumor-specific uptake was validated in an in vitro PDAC model (PANC-1, MDA-MB-231 cells). IGFR overexpression was confirmed in pancreatic cancer cells through western blotting. SDC1.H peptide was conjugated with HiLyte Fluor 555 dye to susbstantiate the tumor-specific uptake via NIR fluorescence imaging. MSOT further confirmed tumor specificity of SDC1.H-750 probe in tissue mimicking phantoms.

Results: Upregulated IGFR expression in pancreatic cancer cells (PANC-1) compared to breast cancer cells (MDA.MB 231) was established through western blotting and immunohistochemistry staining. The uptake of SDC1.H-750 SE probe in PANC-1 cells was upregulated by 2.53–fold in comparison to SDC1-750 SE probe at 500 nM concentration ($p<0.001$) (Figures 1 A & B). Further, SDC1.H-555 SE probe displayed upregulated cellular internalzation in comparison to SDC1-555 SE ($p<0.001$) in both cell lines. MSOT analysis validated higher signal uptake in SDC1.H-750 SE treated cells than commercial SDC1-750 SE.

Conclusion: Enhanced tumor-specificity of SDC1.H-750 probe compared to the commercially available SDC1-750 SE probe establishes a higher dynamic range of SDC1.H peptide for advanced tumor imaging.

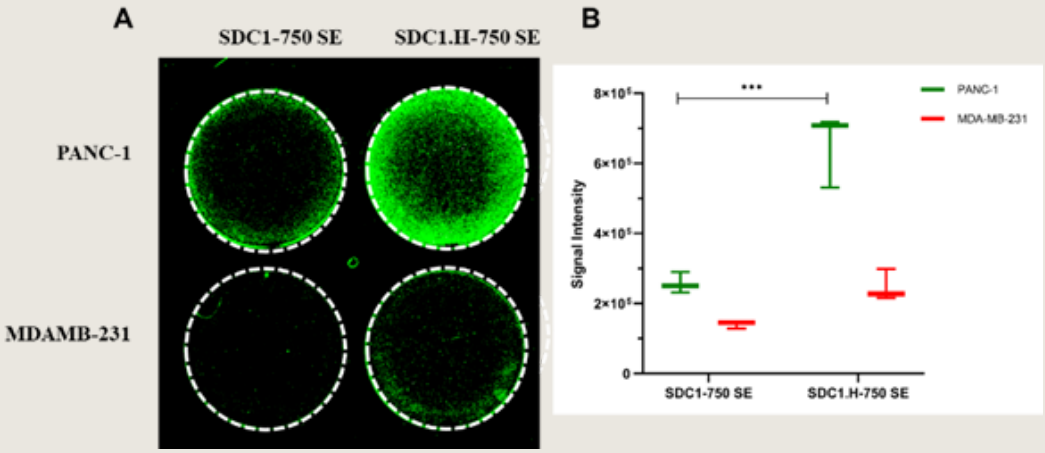

Figure 1. NIR fluorescence confirmation of differential SDC1, SDC1.H uptake in PANC-1 and MDA-MB 231 cells.

References

(1) Beauvais, D. M.; Rapraeger, A. C. Syndecan-1 couples the insulin-like growth factor-1 receptor to inside-out integrin activation. Journal of cell science 2010, 123 (Pt 21), 3796-3807. DOI: 10.1242/jcs.067645.
(2) Kimbrough, C. W.; Hudson, S.; Khanal, A.; Egger, M. E.; McNally, L. R. Orthotopic pancreatic tumors detected by optoacoustic tomography using Syndecan-1. Journal of Surgical Research 2015, 193 (1), 246-254. DOI: 10.1016/j.jss.2014.06.045.

POST DOC

IDENTIFYING CHALLENGES AFTER CHIMERIC ANTIGEN RECEPTOR T-CELL THERAPY: A CONVERGENT MIXED METHODS STUDY

Authors: Aqsa Ashraf MD1, Kira MacDougall MD, MS2, Jennifer Holter Chakrabarty MD1, James George MD1, Sarah Vesely PhD3, Sami Ibrahimi MD1, Dee Terrell PhD3
Affiliations:

1University of Oklahoma Health Science Center
2Christus St. Vincent Regional Cancer Center, Santa Fe, New Mexico
3Hudson College of Public Health

Presenter: Aqsa Ashraf MD, PGY5, Hematology-Oncology

Presentation Preference: Poster

Introduction: Chimeric antigen receptor (CAR) T-cell therapy must be administered at accredited centers. The transition period following CAR-T requires close collaboration between the academic and referring (community) oncologists (CO). Identifying challenges during this period is crucial, yet published studies are limited. This study aims to identify these challenges from both CO and patient perspectives.

Methods: Convergent mixed-methods study was conducted between March-April 2024. The quantitative goal was to identify CO's challenges during the transition period. Eligible oncologists had referred > 1 patient for CAR-T therapy to Stephenson Cancer Center (SCC) (CAR-T center) from 2019-2024. Oncologists completed an online survey ranking the difficulty of various patient care aspects based on hypothetical clinical vignettes. Descriptive statistics were used to describe key challenges. The qualitative goal was to understand patient's challenges. Eligible patients were referred to SCC for CAR-T, > 6 months from CAR-T, and > 18 years old. One-on-one zoom interviews were conducted. Interviews were transcribed verbatim, and themes were identified.

Results: 33/79 (42%) CO completed the study. They belonged to Oklahoma (88%), Texas (6%), Arkansas (3%), and Indiana (3%). 20 patients were interviewed, the mean time to interview was 21 months after CAR-T. 91% CO believed a “Best Practices” handbook would be helpful. CO ranked: 1) understanding which aspect(s) of care now fell under their responsibility (13/32; 41%), and 2) management of relapse (11/29; 40%) as the top challenges. Regarding vaccination after CAR-T, 82% CO agreed CAR-T center determined the vaccination schedule, but only 44% viewed it as the primary administration site. Patient themes were: 1) disease relapse anxiety, 2) perceived communication difficulties between their 2 oncologists, and 3) uncertainty related to the need for re-vaccination.

Conclusion: Our results suggest a dedicated CAR-T clinic would improve patient care and a “Best Practices” handbook or webinar series would benefit CO.

Development of a novel pH low insertion peptide for imaging of pancreatic cancer using multispectral optoacoustic imaging

Ryan C Bynum1*, Emma Sanderson1, Lacey McNally1
1Deparment of Surgery, University of Oklahoma Health Sciences Center, Oklahoma City, OK 73104, USA
* ryan-bynum@ouhsc.edu

Objective: Lack of cancer specific biomarkers in pancreatic cancer is problematic in the development of pancreatic cancer specific imaging. One class of molecules known as pH low insertion peptides (pHLIPs) are of interest here as they allow for the targeting of the acidic microenvironment in pancreatic cancer [1-2]. In developing this novel imaging paradigm using pHLIPs as probes for use with multispectral optoacoustic imaging (MSOT), we have identified a need for a probe with increased dynamic range to further improve imaging accuracy [3]. In this study, we synthesized K7 and the novel pHLIP variant V7FS for use in imaging of pancreatic cancer with improvement in dynamic range.

Methods: K7 and V7FS pHLIP peptides were synthesized using microwave chemistry with >90% purity and conjugated to HiLyte 750 and HiLyte 555 dyes. Peptide-dye bond was confirmed by spectroscopy. pH of human pancreatic tumor and uninvolved tissue were measured intraoperatively using a microsensor. Uptake of K7-750 and V7FS-750 was measured in vitro using near-infrared fluorescent imaging in S2VP10 and S2013 pancreatic cancer cell lines grown in pH specific media (6.6, 6.8, 7.4) in replicates. K7-555 and V7FS-555 were also compared in vitro using flourescent microscopy. Probes were imaged in tissue mimicking phantoms and orthotopic S2VP10 murine model using MSOT. Statistical analysis was performed using ANOVA.

Results: Human pancreatic tumor was more acidic vs uninvolved tissue (pH 6.2-6.7 vs 7.2-7.3, $p<0.01$). V7FS-750 was found to have greater signal when compared to K7-750 at acidic pH ($p<0.05$). At pH 6.6 V7FS-555 had greater signal than K7-555 ($p<0.001$) and V7FS-555 was found to have greater singal intesity at pH 6.6 vs 7.4 ($p<0.01$) on flourescent microscopy. Peak uptake of probe in orthotopic murine models occurred at 3 hours after intravenous injection.

Conclusions: V7FS was shown to be a viable probe for use in the pH targeted imaging of pancreatic cancer cells in vitro. Notably, V7FS was observed to have higher accumulation at more acidic pH when compared to K7. The development of this novel pHLIP probe with increased dynamic range for use in targeted imaging of pancreatic cancer is a valuable step in the development of a pH specific imaging paradigm using MSOT for clinical translation.

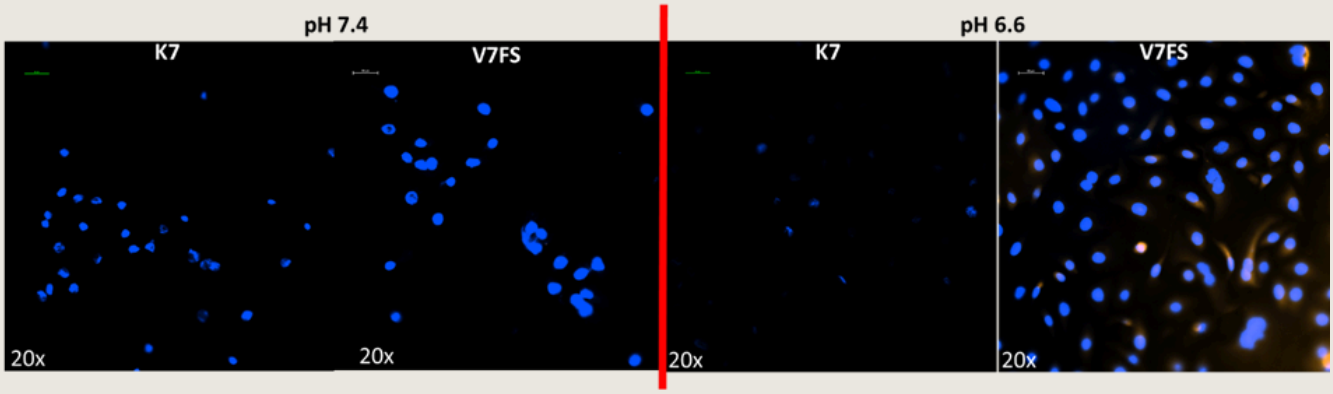

Figure 1. K7-555 vs V7FS-555 at pH 7.4 (left) and pH 6.6 (right).

References

[1] Weerakkody D, Moshnikova A, Thakur MS, et al. Proc Natl Acad Sci U S A. 2013;110:5834-5839.
[2] Reshetnyak YK, Andreev OA, Engelman DM. Front Pharmacol. 2024;15:1355893.
[3] Kimbrough CW, Khanal A, Zeiderman M, et al. Clin Cancer Res. 2015;21:4576-4585.

POST DOC

Preliminary Assessment of the Breast and Prostate Cancer Radiotherapy Carbon Footprint in Ghana through Accessibility to Care

Phylicia D Gawu DO MS1, Charles Akoto-Aidoo BSc2, Isaac J Washburn PhD3, Idalid Franco MD MPH4, Jerry J Jaboin MD PhD MBA1, Aba A Scott MBChB2, Meritxell Mallafre-Larrosa5, Alfredo Polo5, Osama Mohammad MD PhD6, Surbhi Grover MD MBA7, Katie E Lichter MD MPH8, Verna Vanderpuye MBChB FASCO2, Shearwood McClelland III MD1,9

1Depart of Radiation Oncology and 9Neurological Surgery SCC, University of Oklahoma College of Medicine, OKC, OK

2Korle-Bu Radiotherapy Center, Accra Ghana
3Biobehavioral Health Science, University of Oklahoma College of Nursing, Oklahoma City, OK
4Department of Radiation Oncology, Brigham and Women's Hospital, Boston, MA
5City Cancer Challenge, Switzerland; 6Department of Radiation Oncology, MD Anderson Cancer Center, Houston, TX
7Department of Radiation Oncology, University of Pennsylvania, Philadelphia, PA
8Department of Radiation Oncology, University of California at San Francisco, San Francisco, CA
Phylicia.gawu@ouhsc.edu

Purpose/Objective(s):
With rising cancer rates among minority populations and growing climate concerns, a comprehensive lifecycle assessment (LCA) of external beam radiotherapy (EBRT) in Ghana was conducted to estimate its environmental impact, adapting recent findings from the U.S. to a global context.

Materials/Methods:
Following ISO 14040 and 14044 standards, this LCA focuses on breast and prostate cancer patients receiving EBRT at Korle-Bu Teaching Hospital (KBTH), Ghana. Data included patient travel, staff travel, and treatment regimens for comparisons to U.S.-based data.

Results:
The final analysis included five breast cancer patients treated between 2023 and 2024. Four patients received 50 Gy in 25 fractions, while one patient received 40.05 Gy in 15 fractions, with all treatments delivered using a cobalt machine. In contrast, five prostate cancer patients, treated in 2023, were treated on a linear accelerator (linac). Four of these patients received 78 Gy in 39 fractions, and one followed a 40-fraction regimen.
Breast cancer patients traveled an average of 27.8 km (17.3 mi) for their initial consultation, with a median distance of 18.7 km (11.6 mi). The average distance traveled by clinic staff—comprising the biostatistician, nurse, health assistant, and oncologist—was 40.8 km (25.4 mi), with a median distance of 10.1 km (6.3 mi).

During the treatment phase, breast cancer patients traveled an average of 9.3 km (5.8 mi), with a median distance of 5.3 km (3.3 mi). Radiation therapists traveled an average of 10.6 km (6.6 mi) during this period, with a median of 8.5 km (5.3 mi).
Prostate cancer patients traveled an average of 22.6 km (14.0 mi) for consultation, with a median distance of 18.8 km (11.7 mi). Clinic staff attending to prostate cancer patients had an average travel distance of 42.9 km (26.7 mi) and a median of 10.1 km (6.3 mi).
During the treatment phase, prostate cancer patients traveled an average of 23.4 km (14.5 mi), with a median distance of 20.2 km (15.6 mi). Radiation therapists traveled an average distance of 22.4 km (13.9 mi) during the treatment course, with a median of 31.9 km (19.8 mi).

Conclusion:
The feasibility of conducting LCAs in Ghana is confirmed, with initial results showing distinct travel patterns for patients and staff compared to U.S. benchmarks. Future expansion to additional disease sites will offer a fuller view of EBRT’s environmental impact in Ghana.

References

1. Lichter KE, Charbonneau K, Lewy JR, Bloom JR, Shenker R, Sabbagh A, Chino J, Rodrigues A, Hearn J, Grover S, Sheu RD, Witztum A, Qureshi MM, Yom SS, Anand C, Thiel CL, Mohamad O. Quantification of the environmental impact of radiotherapy and associated secondary human health effects: a multi-institutional retrospective analysis and simulation. Lancet Oncol. 2024 Jun;25(6):790-801. doi: 10.1016/S1470-2045(24)00148-7. PMID: 38821084.

2. Lichter KE, Charbonneau K, Sabbagh A, Witztum A, Chuter R, Anand C, Thiel CL, Mohamad O. Evaluating the Environmental Impact of Radiation Therapy Using Life Cycle Assessments: A Critical Review. Int J Radiat Oncol Biol Phys. 2023 Nov 1;117(3):554-567. doi: 10.1016/j.ijrobp.2023.04.036. Epub 2023 May 11. PMID: 37172916.

3. ISO I. Environmental Management–Life Cycle Assessment–Requirement an d Guidelines. S2006b ISO. 2006;14044.

Repurposing Mebendazole to Combat Chemoresistance in Ovarian Cancer:

Penta Dhanamjai1, Dey Debasish K1, Benbrook Doris M1, Wang Lin2, Bieniasz Magdalena2, Chandra Vishal1, Dockery LE1#, Rai Rajani1#

1Gynecologic Oncology Section, Obstetrics and Gynecology Department, Stephenson Cancer Center, University of Oklahoma Health Sciences Center, Oklahoma City, OK 73104, USA.

2Patient-Derived Xenograft and Preclinical Therapeutics Core facility, Aging and Metabolism Program, Oklahoma Medical Research Foundation, Oklahoma City, OK, USA

Email Address: Dhanamjai-Penta@ouhsc.edu, rajani-rai@ouhsc.edu

Abstract

Introduction: Ovarian cancer (OvCa) is a highly aggressive gynecological malignancy, often associated with a metastatic phenotype, chemoresistance, and recurrence. Despite the initial positive clinical response to frontline platinum-based therapies, up to 80% of OvCa patients eventually relapse, become platinum unresponsive, and develop metastatic dissemination via spheroids in the ascitic fluid. Although maintenance therapy has added clinical benefits, it has considerable toxicity, high cost, and limited response rates. Therefore, there is a pressing need to develop new, effective, low-toxicity treatments to overcome relapse and chemoresistance in OvCa. Repurposing existing drugs is an increasingly popular strategy in oncology due to the financial and logistical constraints of new drug development. Recently, the anti-parasitic drug mebendazole (MBZ) has emerged as a promising repurposed oncology drug, showing potential in treating multiple types of tumors. In this study, we examined the efficacy of MBZ against cisplatin-resistant OvCa.

Methods: The in vitro efficacy of MBZ was evaluated in cisplatin-resistant (CPR) and parent (WT/sensitive) human OvCa OVCAR-8 cell lines, as well as in ascites samples collected from chemoresistant OvCa patients, using 2D and 3D cell viability assays and invasion assays. The preclinical efficacy of MBZ was assessed in orthotopic animal model utilizing CPR-OVCAR-8 spheroids, and patient-derived xenograft (PDX) animal model with specimens from chemo refractory OvCa patients. Molecular mechanisms were investigated through western blot and immunofluorescence analysis.

Results: MBZ efficiently decreased cell viability, spheroid size, and the invasion ability of OvCa cell lines and ascites samples. OvCa cells treated with MBZ demonstrated downregulation of proliferation markers and upregulation of apoptosis markers, indicating inhibition of cell proliferation and induction of apoptosis. A low dose of MBZ inhibited the spheroid invasion of both OVCAR-8 CPR and ascites-derived cells from patients by regulating the epithelial-mesenchymal transition (EMT). Mechanistically, MBZ inhibited the Wnt/β-catenin signaling pathway by downregulating the expression and nuclear localization of β-catenin phosphorylated at Ser552 and Ser675, which are known to promote the transcriptional activity of β-catenin. Preclinical studies showed that MBZ at a dose of 50 mg/kg/day for 28 days significantly reduced tumor growth in PDX and orthotopic tumor models without any evidence of toxicity.

Conclusion: Collectively, our study strongly supports the therapeutic potential of MBZ against chemoresistant OvCa, justifying further mechanistic studies, drug dosing optimization, and combination therapy investigations.

Keywords: Ovarian Cancer, Wnt/β-catenin pathway, Mebendazole.
Acknowledgment of Funding: The work is supported by COBRE P20GM135009, and was supported by the PHF Clinician Scientist Development Grant Program.

Keywords: Ovarian Cancer, Wnt/β-catenin pathway, Mebendazole.
Acknowledgment of Funding: The work is supported by COBRE P20GM135009, and was supported by the PHF Clinician Scientist Development Grant Program.

POST DOC

Regulating IL-1β to Enhance Patient Outcomes by reducing Myelopoiesis and Immune Suppression in Glioblastoma

Presenting Author1*, Saeede Soleimanian
Co-authors2 Subhajit Ghosh, Tae Gyu Oh, Jiayi Huang, Jerry Jaboin, Dinesh Thotala*

1Department of Radiation Oncology, Oklahoma University Health Sciences Center, Oklahoma City, Oklahoma, USA
Department of Radiation Oncology, Washington University School of Medicine, St. Louis, MO, USA.
* dinesh-thotala@ouhsc.edu

Background: In clinical trials, we found elevated IL-1β levels in plasma and a corresponding increase in circulating MDSCs in lymphopenic GBM patients. TCGA data showed that GBM patients with high IL-1β expression had worse outcomes than those with low expression. The role of IL-1β in GBM progression remains unclear, but its increased expression may modulate immune responses in the tumor microenvironment and promote immune suppression. Our research explores IL-1β's role in radiation-induced MDSC expansion and its effects on immune suppression and prognosis in GBM.

Methods: To evaluate the role of IL-1β in radiation-induced immunosuppression we comprehensively analyzed circulating immune cells and pro-inflammatory cytokines in GBM patients undergoing chemoradiotherapy. Using an orthotopic mouse model of GBM, we evaluated the impact of IL-1β on survival, immune organs, and tumors. Multi-color flow cytometry was employed for immune profiling, and functional assays were utilized to measure MDSC expansion.

Results: We found that radiation increased IL-1β levels in the serum of both GBM patients and mice. In mice with orthotopic GBM, radiation-induced IL-1β led to hematopoietic stem cell (HSPC) differentiation towards myeloid cells (myelopoiesis), resulting in a surge of MDSC precursor cells in the bone marrow and increased MDSCs in peripheral blood and the tumor microenvironment (TME). Exogenous IL-1β administration in mice confirmed its crucial role in myelopoiesis. Targeting IL-1β reduced HSPC myelopoiesis. Targeting both IL-1β and MDSCs reduced MDSC levels and increased CD8 T cell infiltration in the tumor microenvironment, leading to extended survival in GBM-bearing mice.

Conclusions: Our study demonstrates that radiation-induced elevation of IL-1β levels promotes myelopoiesis, increasing MDSC precursor cells in the bone marrow and their accumulation in peripheral blood and the TME. Targeting IL-1β effectively reduces myelopoiesis, enhances CD8 T cell infiltration in the TME, and prolongs the survival of GBM-bearing mice. These findings underscore the potential therapeutic significance of IL-1β modulation.

POST DOC

Title: Enhancing Immunotherapy Efficacy in Glioblastoma by Targeting CXCR1/2-Mediated Immunosuppression

Presenting Author1*: Sandeepkumar Sriramanujam
Co-authors1 Saeede Soleimanian, Subhajit Ghosh, Jerry Jaboin, Dinesh Thotala*

1Department of Radiation Oncology, Oklahoma University Health Sciences Center, Oklahoma City, Oklahoma, USA
Department of Radiation Oncology, Washington University School of Medicine, St. Louis, MO, USA.

Abstract:
Background: Glioblastoma (GBM), the most common and aggressive brain tumor, has a median survival of just 14–16 months despite surgery, radiation, and temozolomide (TMZ). Checkpoint inhibitors, effective in other cancers, have shown limited success in GBM due to high levels of regulatory T cells and myeloid-derived suppressor cells (MDSCs), which suppress immune responses. We found immunosuppressed GBM patients had elevated MDSCs with increased CXCR2 expression. Our research focuses on the role of CXCR2 in radiation-induced MDSC expansion and its impact on immune suppression and prognosis in GBM.

Methods: Using an orthotopic GBM mouse model, we evaluated the effects of targeting CXCR1/2 in combination with radiation and anti-PD-1, on survival, immune organ dynamics, and tumor progression. The study included comprehensive immune profiling using multi-color flow cytometry, along with functional assays to evaluate MDSC expansion.

Results: In a syngeneic orthotopic mouse (C57BL/6) GBM (GL261) model, we found that fractionated RT (2 Gy for 5 consecutive days) resulted in a decrease in CD4/CD8 T cells and an increase in MDSCs compared to sham-irradiated mice. MDSCs from irradiated mice also showed elevated CXCR2 expression. Our findings further revealed that G-MDSCs play a key role in the immunosuppressive tumor microenvironment, and their inhibition restores T-cell function and improves survival outcomes. Targeting CXCR1/2 with the small molecule inhibitor SX-682 significantly reduced MDSC recruitment. Additionally, combining SX-682 with anti-PD-1 (αPD-1) therapy enhanced T-cell activation and extended survival in preclinical studies.

Conclusion: Our syngeneic orthotopic GBM mouse model demonstrated that radiation therapy exacerbates this immunosuppression by increasing MDSC populations and reducing T-cell activity. However, targeting CXCR1/2 with the small molecule inhibitor SX-682 effectively reduced MDSC recruitment and restored T-cell functionality. The combination of SX-682 with anti-PD-1 therapy further amplified T-cell activation and prolonged survival in preclinical models, offering a promising therapeutic strategy for overcoming immune suppression and improving treatment outcomes in GBM.

Design and Synthesis of Azo Dyes with Coumarin Thiophene for pH and Hydroxide Sensing Applications

Mohamed Yahya and Lacey R. McNally
Stephenson Cancer Center, University of Oklahoma Health Science, Oklahoma City, Oklahoma, USA
E-mail : Mohamed-yahya@ouhsc.edu and lacey-mcnally@ouhsc.edu

Azo dyes are employed in advanced applications such as lasers and nonlinear optical (NLO) systems due to their stability and optical properties [1]. Recent studies have focused on developing cost-effective chemosensors for detecting cations and anions, which change color or emission upon interaction with specific substrates [2]. Proton-sensitive azo dyes are particularly valuable for pH sensing, addressing the limitations of traditional glass electrodes. Azo dyes containing coumarin thiophene have gained attention for their potential in sensing and NLO applications [3]. with intramolecular charge transfer contributing to their photophysical properties.

The objective of this study is to design and synthesize a visual chemosensor for pH and hydroxide detection. To achieve this, three novel azo dyes bearing coumarin thiophene were synthesized and characterized using 1H NMR, 13C NMR, IR, UV–vis, and HRMS techniques. The effect of different solvents with varying dielectric constants (ε) on UV–vis absorption was investigated. The acidochromic properties, reversibility, and hydroxide sensing capabilities of the products were also examined. Finally, the second-order NLO properties and thermal stabilities of the products were studied.

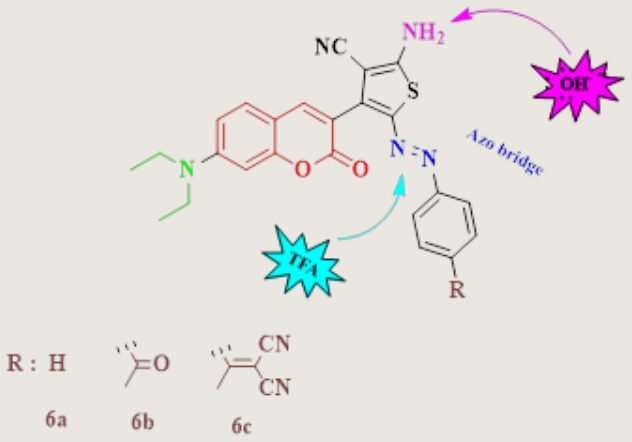

Scheme 1. Efficient Synthesis and Properties of Coumarin-Thiophene Azo Dyes

References

[1] M. Yahya, R. Metin, B. Aydıner, N. Seferoğlu and Z. Seferoğlu, Anal. Sci., 2023, 39, 829–842
[2] M. Yahya, N. Seferoğlu, G. Kaplan, Y. Nural, A. Barsella and Z. Seferoğlu, , J. Mol. Struct., 2023, 1273,
[3] I. Yahaya, E. Keleş, A.Putra, M. Yahya, N. Seferoğlu and Z. Seferoğlu, J. Mol. Struct., 2020, 1204, 127465

Balancing your merits: pH sensitive hemicyanine fluorophores for both fluorescence and photoacoustic imaging

Tarek Erfan Ahmed1*, Maged Henary*1,2
1Department of Chemistry, Georgia State University, Atlanta, Georgia, 30303
2Center For Diagnostics and Therapeutics, Georgia State University, Atlanta, Georgia, 30303
* tahmed13@student.gsu.edu

Abstract
Photoacoustic imaging has gathered the interest of biomedical imaging community due to its unique capabilities of deeper tissue penetration and high spatial resolution1, 2. Despite these advantages, fluorescence imaging still holds its attraction due to the high sensitivity and specificity that can be achieved through it3. Our lab has developed a scaffold of hemicyanine fluorophores with the xanthene ring in order to be used for photoacoustic imaging4. They showed strong photoacoustic signals with unique shape and strength, but their fluorescence signal was not very high. The design of fluorophores that can be used in both fluorescence and photoacoustic modalities will be advantageous in combining the benefits of both methods5. Herein, the design and synthesis of a series of hemicyanine fluorophores with the thioxanthene ring is described. The presence of sulfur atom in the thioxanthene ring not only causes a bathochromic shift in the absorbance and fluorescence wavelengths, but also helps to balance the relaxation pathways allowing for both radiative and non-radiative decays which enables both fluorescence and photoacoustic imaging. The optical properties of the synthesized hemicyanine fluorophores were studied, and they exhibited high molar extinction coefficient and good molecular brightness. Moreover, their absorbance was studied in buffer solution at different pH values to mimic the different environments inside the body. They showed a ratiometric response by changing the pH with a calculated pKa value of 6.03. The unique scaffold of the synthesized hemicyanine fluorophores with their promising optical properties and pH sensitivity make them strong candidates for dual fluorescence and photoacoustic imaging and paves the way towards further optimization for more biomedical applications.

References
(1) Laramie, M. D.; Smith, M. K.; Marmarchi, F.; McNally, L. R.; Henary, M. Small molecule optoacoustic contrast agents: an unexplored avenue for enhancing in vivo imaging. Molecules 2018, 23 (11), 2766.
(2) St. Lorenz, A.; Buabeng, E. R.; Taratula, O.; Taratula, O.; Henary, M. Near-infrared heptamethine cyanine dyes for nanoparticle-based photoacoustic imaging and photothermal therapy. Journal of medicinal chemistry 2021, 64 (12), 8798-8805.
(3) Owens, E. A.; Henary, M.; El Fakhri, G.; Choi, H. S. Tissue-specific near-infrared fluorescence imaging. Accounts of chemical research 2016, 49 (9), 1731-1740.
(4) Gardner, S. H.; Brady, C. J.; Keeton, C.; Yadav, A. K.; Mallojjala, S. C.; Lucero, M. Y.; Su, S.; Yu, Z.; Hirschi, J. S.; Mirica, L. M. A general approach to convert hemicyanine dyes into highly optimized photoacoustic scaffolds for analyte sensing. Angewandte Chemie International Edition 2021, 60 (34), 18860-18866.
(5) Zhang, S.; Chen, H.; Wang, L.; Qin, X.; Jiang, B. P.; Ji, S. C.; Shen, X. C.; Liang, H. A general approach to design dual ratiometric fluorescent and photoacoustic probes for quantitatively visualizing tumor hypoxia levels in vivo. Angewandte Chemie 2022, 134 (7), e202107076.

Acknowledgements
The author wishes to thank his advisor Dr. Maged Henary for his continuous guidance and support during this project. I would also like to thank the department of Chemistry at Georgia State University for supporting my Ph.D. program.

STUDENT

Title: ACSS2 mediates the crosstalk between cancer cachexia and immune evasion through IL-15 in pancreatic cancer

Yang Cai,1,2 Zhijun Zhou,1,2 Xiuhui Shi,1,2 Mingyang Liu,1,2 Alex X. Arreola,1,3 Jingxuan Yang,1,2 Yu Ren,1,2 Michael S. Bronze,1 Courtney W. Houchen,1 Yuqing Zhang,1,2 Min Li,1,2
1Department of Medicine, The University of Oklahoma Health Sciences Center, Oklahoma City, OK 73104, USA
2Department of Surgery, The University of Oklahoma Health Sciences Center, Oklahoma City, OK 73104, USA
3Department of Pathology, The University of Oklahoma Health Sciences Center, Oklahoma City, OK 73104, USA

Introduction
Cancer cachexia and immune evasion are two hallmarks of pancreatic cancer. Yet little is known about how these two features coordinate in pancreatic cancer. Acetyl-coenzyme A synthetase 2 (ACSS2) promotes metabolic reprogramming and cancer cachexia. This study aimed to dissect the underlying mechanism of ACSS2-mediated interplay between cancer cachexia and immune evasion in pancreatic cancer.

Methods
We investigated the association between cancer cachexia and treatment response to immunotherapy in several cohorts of patients with different cancer types. In silico analysis, in vitro experiments and orthotopic mouse model were utilized to reveal the mechanism of the interaction between cancer cachexia and immune evasion in pancreatic cancer.

Results
The treatment response to immunotherapy decreased in patients with cancer cachexia. The level of IL-15 in muscle tissue is higher in mice without cancer cachexia compared to those with cancer cachexia. High IL-15 level is associated with better treatment outcomes for patients who receive immunotherapy. Mechanistically, IL-15 promotes tumor immune surveillance by increasing immune infiltration, upregulating IFN-γ signaling axis, and decreasing immunosenescence in tumor microenvironment. ACSS2 induced tumor immune evasion by decreasing IL-15 level in muscle tissue and tumor tissue. Blockage of ACSS2 restored the level of IL-15 and attenuated muscle wasting and tumor immune evasion.

Conclusion

This study reveals a previously uncharacterized role of ACSS2 on immune evasion. Specifically, ACSS2 promotes the interaction between immune evasion and cancer cachexia through IL-15 mediated immunosenescence, thus providing novel therapeutic targets for cancer cachexia and immune evasion in pancreatic cancer.

DEVELOPMENT OF A NOVEL PANCREATIC IMAGING PROBE USING CLAUDIN-4

Olivia Chakrabarty1, Ryan Bynum1, Karl N Thomas1 Emma Sanderson1, Barish Edil1, Molly McNally1 Lacey Mcnally1
1Stephenson Cancer Center, University of Oklahoma, Oklahoma City, OK
* oliviaic28@gmail.com

Abstract: Pancreatic cancer remains one of the most lethal malignancies, with high mortality rates and a significant survival advantage associated with complete surgical resection. In this study, we present a novel Claudin-4 probe designed for intraoperative detection of pancreatic cancer, aimed at improving surgical margin identification. Claudin-4 is a tight junction protein that is overexpressed in various cancers, including pancreatic cancer. We developed a fluorescent imaging agent by conjugating a 750 nm fluorescent dye to the amine terminus of a previously characterized long sequence of Claudin-4. Confirmation of conjugation was achieved via spectrophotometry, revealing a peak absorbance at 756.6 nm.

Subsequent binding assays with the S2VP10 pancreatic cancer cell line demonstrated visually enhanced binding of the Claudin-4 probe, with quantitative analysis showing increased binding in correlation with probe concentration. The probe's binding affinity was further assessed across three pancreatic cancer cell lines: MiaPaca, S2VP10, and Panc1, at 0 and 10 µM concentrations. While all three lines exhibited Claudin-4 binding, MiaPaca showed the highest expression levels. Western blot analysis confirmed the presence of significant Claudin-4 protein across all tested cell lines

These findings suggest that the developed Claudin-4 probe effectively identifies pancreatic cancer cells, supporting its potential application in intraoperative settings to delineate tumor margins. This novel imaging agent could enhance surgical outcomes by ensuring more accurate tumor resections and ultimately improving patient survival rates. Further in vivo studies will be required to evaluate the probe's efficacy in clinical applications.

References

1. Wang C, Wu N, Pei B, Ma X, Yang W. Claudin and pancreatic cancer. Front Oncol. 2023 Mar 7;13:1136227. doi: 10.3389/fonc.2023.1136227. PMID: 36959784; PMCID: PMC10027734.
2. Kojima T, Kyuno D, Sawada N. Targeting claudin-4 in human pancreatic cancer. Expert Opin Ther Targets. 2012 Sep;16(9):881-7. doi: 10.1517/14728222.2012.708340. Epub 2012 Jul 16. PMID: 22800288.
3. Bang C, Park MG, Cho IK, Lee DE, Kim GL, Jang EH, Shim MK, Yoon HY, Lee S, Kim JH. Liposomes targeting the cancer cell-exposed receptor, claudin-4, for pancreatic cancer chemotherapy. Biomater Res. 2023 May 26;27(1):53. doi: 10.1186/s40824-023-00394-7. PMID: 37237291; PMCID: PMC10214683.

Acknowledgements
The author wishes to thank the McNally Lab for the summer internship opportunity

STUDENT

Targeting EMMPRIN With S100A9-750 Probe to Image Pancreatic Ductal Adenocarcinoma

Barish H. Edil Jr., Ryan C. Bynum, Rohit Singh, Happy Agarwal, Molly W. McNally, Karl N. Thomas, Emma J. Sanderson, Lacey R. McNally
University of Oklahoma Health Sciences Center
Barish-EdilJr@ouhsc.edu

Abstract

Introduction: Pancreatic ductal adenocarcinoma, PDAC, remains a recalcitrant cancer. While 15-20% of patients are eligible for surgical resection, up to 70% of resectable patients have positive margins. Extracellular matrix metalloproteinase inducer, EMMPRIN/CD147, is a membrane-bound glycoprotein, highly expressed on most cancer cells, but has limited expression in normal cells. Using an S100A9 ligand, we developed an EMMPRIN targeted probe to visualize pancreatic tumor cells via NIR fluorescence imaging.

Methods: Pancreatic adenocarcinoma cancer cell lines, MiaPaca2, Panc1, Suit2, S2VP10 and S2013 were assessed for EMMPRIN by western blotting. The S100A9 peptide was synthesized using microwave chemistry and lyophilized. Hilyte-750 succinimidyl ester and Hilyte-750 amine reactive dyes were independently conjugated to the S100A9 peptide to determine the optimal orientation of the dye. Successful conjugation was confirmed using spectroscopy. Binding of 750-S100A9 (N-terminal) and S100A9-750 (C-terminal) probes to PDAC cells was determined using NIR imaging and in tissue mimicking phantoms via multispectral optoacoustic tomography (MSOT) imaging.

Results: MiaPaca2, Panc1, and S2013 had high EMMPRIN expression while Panc1 and S2VP10 had lower expression. Successful conjugation of peptide to reactive dyes resulted in an OD of 0.1 each. Initial testing of N-terminal and C-terminal conjugated S100A9 probes showed that C-terminal conjugated S100A9 resulted in higher signals of 279,600 a.u. at 500 nM vs. 4,055 a.u. of N-terminal 750-S100A9 in S2VP10 ($p < 0.05$). Tissue mimicking phantoms showed increased signal of C-terminal S100A9-750 at 22.4 a.u vs < 0.001 a.u. in N-terminal probe in S2VP10 by MSOT imaging. Shrinking S100A9 peptide to 89 amino acids demonstrates the highest signal in the cancer cells versus full-length peptide.

Conclusion: EMMPRIN/CD147 demonstrates to be a suitable target for PDAC using an S100A9 ligand conjugated near infrared fluorescent dye to the C-terminal end of the peptide. Our findings suggest that S100A9 could increase PDAC specificity for either contrast agents or potentially for nanoparticles.

STUDENT

Positively Charged NIR Fluorophores for Cartilage Targeting

Guliz Ersoy Ozmen,1 Homan Kang,2, * Seung Hun Park,2 Jason Dinh,1Haoran Wang,2 Won Hur,2 Vy Nguyen,2 Sung Ahn,2 Atsushi Yamashita,2 Wesley R. Stiles,2Satoshi Kashiwagi,2 Kai Bao,2 Hak Soo Choi2 and Maged Henary,1, 3

1Department of Chemistry, Molecular Basis of Disease, Georgia State University, Atlanta, GA 30303, USA
2 Gordon Center for Medical Imaging, Department of Radiology, Massachusetts General Hospital
and Harvard Medical School, Boston, MA 02114, USA
1Department of Chemistry, Center of Diagnostics and Therapeutics, Georgia State University, Atlanta, GA 30303, USA
* mhenary1@mail.com

Early diagnosis is crucial for the effective treatment of rheumatoid arthritis because continuing inflammation can lead to irreversible joint damage and disability. However, current diagnostic methods lack tissue-specific guidelines to monitor the progressive course of degenerative joint diseases. Cyanine dyes have been known for a long time and used for both fluorescence and photoacoustic imaging. One of the most used cyanine dyes is indocyanine green (ICG) which has absorbance and fluorescence in NIR region. This region is known as the therapeutic window since biomolecules in human body and the skin has less autofluorescence and NIR light can penetrate deeper into the tissue.

Here, we report the synthesis of new cyanine dyes modified at the meso position with thiochlorine moiety to introduce three positive charges to introduce cartilage targeting ability to compounds in the near-infrared-II (NIR-II) window. Due to the negatively charged nature of cartilage tissue, the positively charged molecules have shown better targeting ability. The synthesized compounds were characterized by 1H, 13C NMR and high-resolution mass spectroscopy. They have minimal tissue scattering and negligible autofluorescence. The fluorophores have shown little to no toxicity, both in vitro (up to 100 µM) and in vivo (3 µmol/kg via intravenous injection), suggesting clinical potential. Furthermore, the NIR-II window enable the precise visualization of cartilage lining, serving as a reliable diagnostic indicator for the early detection of arthritis in preclinical mouse models. These fluorophores are NIR fluorescence-emitting targeted contrast agents for prognostic imaging of joint tissue, with the potential biomedical applications

STUDENT

Title: A method for generation of Conditional degron tags (CDTs) knockins for the cell-line with limited homology-directed repair capacity

Presenter: Beibei Liu

Additional Authors: Dr. Tomoharu Kanie

Mentor: Dr. Tomoharu Kanie

Affiliations: Department of Cell Biology

Targeted protein degradation using conditional degron tags (CDTs) technologies are powerful methods for post-translational manipulation of protein levels to investigate biological function. CDTs are valuable tools for rapid degradation kinetics, reversible recovery of protein levels after drug removal, and orthogonal and/or known off-target effects of the degrader drug. But finding the right tag for a protein of interest (POI) can often be an ad hoc and iterative process. Most previous studies either utilized the cell lines with high homologous recombination rates or express the exogenous POI to facilitate and simplify the generation process of knock-ins. The hTERT-RPE1 is genetically stable near diploid cell commonly used to model ciliogenesis, cell division, or DNA repair in a non-transformed context. When applying different CDTs to hTERT-RPE1 cells, we have found highly variable results, which significantly impacted our ability to use CDTs for our studies. Several possibilities of this problem: (1) the poor transfectability and limited homology-directed repair capacity of hTERT-RPE1 hamper their amenability to gene editing; (2) the expression levels of endogenous POIs are variable; (3) each POI requires a unique strategy, thus, requiring a systematic assessment of multiple CDT strategies. Here, we describe a method for rapid and efficient generation of diverse heterozygous CDTs knock-ins. In contrast to other approaches, this strategy bypasses the need for single cell cloning. Our approach can also be applied to a variety of cell types with poor transfectability and limited homology-directed repair capacity

Disease Outcomes for Early Stage Oral Cavity Cancer with WPOI-5 Treated With or Without Post-Operative Radiation Therapy

Patricia Pius1, Casey Buller1, Paul Pitts1, Alekhya Mitta1, Lauren Olay 1, Hayden Jackson 1, Timothy Malouff1, Brian Besch2, Greg Krempl3, Rusha Patel3, and Christina Henson1
1University of Oklahoma Health Sciences Center, Department of Radiation Oncology
2University of Oklahoma Health Sciences Center, Department of Pathology
3University of Oklahoma Health Sciences Center, Department of Otolaryngology
patricia-pius@ouhsc.edu

Introduction: There are several pathologic risk factors that influence post- operative management of early-stage oral cavity squamous carcinoma (OSCC). The worst pattern of invasion (WPOI), ranging from I-V, is a known prognosticator for OSCC, specifically WPOI-5. Because it remains optional in pathology reporting, it is not widely utilized to guide adjuvant therapy of early stage OSCC. Our study aims to analyze clinical outcomes with early stage OSCC and WPOI-5 to determine whether WPOI-5 is an indication for adjuvant radiation therapy (RT) in this population.

Methods and Materials: This is a single- institution retrospective analysis of patients with early-stage OSCC (T1-2 Nx-N0 M0) and WPOI-5 who were either observed or treated with adjuvant radiation therapy. WPOI-5 was defined as tumor dispersion >/=1mm between tumor satellites. Tumor stage, per the AJCC 8th edition, and histopathological features were collected from pathology reports at the time of initial surgery. Electronic medical records were used to collect information regarding patient demographics, adjuvant treatment and disease status. Median follow-up was defined as time from initial surgery to most recent follow-up. Median progression free survival (PFS) was defined as time from initial surgery to time of disease progression.

Results: We identified 10 patients meeting the inclusion criteria treated between December 2018 and February 2024 at our institution. Median follow-up time was 16.8 months. All patients underwent partial glossectomy, and 5 patients underwent neck dissection at the time of initial surgery. All tumors had negative margins. 6 tumors demonstrated perineural invasion and none demonstrated lymphovascular invasion. Following surgery, 4 patients were observed and 6 underwent adjuvant RT. RT dose was 60 Gy in 30 fractions. None of the patients received chemotherapy. At time of last follow up, 9 patients were alive and under active surveillance. Median progression free survival was 6.2 months in the observation cohort versus not reached in the adjuvant RT cohort. 3 out of the 4 patients in the observation arm had recurred at time of analysis and all recurrences were locoregional. Additionally, one of these patients died due to disease progression. There have been no locoregional or distant recurrences in the adjuvant RT cohort.

Conclusion: While our study is limited by small sample size, it demonstrates the impact of high risk WPOI on tumor behavior and disease outcomes. Additionally, the presence of WPOI-5 in early stage OSCC might be more relevant than historic poor prognostic factors, and this patient population may benefit from adjuvant radiation. A larger, multi-institutional retrospective analysis is required to further investigate this trend.

References

Huang SH, O'Sullivan B. Oral Cancer: Current Role of Radiotherapy and Chemotherapy. Med Oral Patol Ora Cir Bucal 2013; 2: 233-240

Langedijk JA, De Jong MA, Leemans CHR, et al. Postoperative Radiotherapy in Squamous Cell Carcinoma of the Oral Cavity: The Importance of the Overall Treatment Time. Int. J. Radiation Oncology Biol. Phys 2003; 57(3): 693-700

Li Y, Bai S, Carroll W, et al. Validation of the Risk Model: High-Risk Classification and Tumor Pattern of Invasion Predict Outcome for Patients with Low-Stage Oral Cavity Squamous Cell Carcinoma. Head and Neck Pathol 2013; 7:211-223

Acknowledgements

The author wishes to thank Dr. Christina Henson

STUDENT

Title: Temporally Multiplexed Imaging of Cell Cycle Dynamics Using Reversibly Photoswitchable Fluorescent Proteins in FUCCI4 Cells

Cilia are evolutionary conserved organelles that extend from the centriole. The cilium cycles assembly and disassembly depending on the cell-cycle; the formation of the cilium typically occurs during G0/G1 phase of the cell cycle, whereas the cilium is disassembled prior to mitosis, as centrioles participate in spindle formation. Our research focuses on imaging the entire process of the cilium formation to understand how ciliary/centriolar proteins orchestrate to form the cilium in coordination with the cell cycle. To visualize the complexed protein dynamics, we seek to establish a method that allows us to simultaneously image a dozen of ciliary/centriolar proteins using the recently developped Temporally Multiplexed Imaging (TMI) technique (PMID: 38029746). This novel approach utilizes reversibly photoswitchable fluorescent proteins (rsFPs) with distinct off-switching rates. The combined spectrally similar signal with different photoswitching kinetics can be unmixed into a linear combination of the kinetics from each fluorophore, which allows concurrent visualization of more than four fluorophores, a typical limit of the standard microscope. To prove the concept of TMI using Fluorescent Ubiquitination-based Cell Cycle Indicator 4 (Fucci4), I generated cell lines stably expressing four cell cycle markers (Cdt1, Geminin, SLBP, and Histon H1), each of which is tagged with a different photoswitchable protein with similar excitation/emission spectra. I then performed live-cell imaging and analyzed the data using MATLAB-based linear algebra techniques and least squares regression for unmixing. In this presentation, I will show the data from my recent experiments, and discuss challenges toward successful visualization of ciliogenesis process using the TMI technologies.

STUDENT

Emma Sanderson1, Ryan Bynum2, Tereza Husarova3, Lacey McNally4
1 Department of Chemistry, University of Oklahoma
2 Department of Surgery, University of Oklahoma Health Science Center
3 Department of Surgery, Military Hospital Prague, Czech Republic
4 Department of Surgery, University of Oklahoma Health Science Center

Background: Pancreatic ductal adenocarcinoma (PDAC) is generally detected late and patients have poor outcomes. Current methods to identify pancreatic cancer generally involve 3D imaging techniques such as CT. However, CT has inferior resolution and often is unable to differentiate live pancreatic tumors from fibrosis. To overcome these limitations, we employed optoacoustic imaging combined with the pH-sensitive peptide probe, V3, to identify pancreatic cancer in orthotopic mouse models.

Methods: We utilized microwave chemistry to synthesize the V3 peptide or V3FS, resulting in a purity of greater than 90%. The V3 or V3FS peptide was then conjugated to a fluorescent dye and dialyzed to make the V3-750 or V3FS-750 probe. S2VP10 and S2013 pancreatic cancer cell lines were plated in 6-well plates and acclimated to 7.4, 6.8, and 6.6 to mimic the healthy cell microenvironment and the pancreatic cancer cell microenvironment. Cells were treated with 1 micromolar of the V3-750 or V3FS-750 probe for 1 hour, then imaged with the near-infrared (NIR) fluorescence imager. Cells were then scraped and loaded into tissue mimicking phantoms and imaged with multispectral optoacoustic tomography (MSOT). Athymic mice were orthotopically injected with S2VP10 cells and tumors grew to 3 mm. The V3-750 or V3FS-750 probes were intravenously injected, and mice were imaged 3h post-injection with MSOT.

Results: NIR fluorescence signal values for the samples displayed a trend that the V3-750 and V3FS-750 probes targeted 6.6 and 6.8 pH environments more than the 7.4 pH environment. MSOT data supported this trend, with the signal values from 6.6 and 6.8 pH being greater than the 7.4 pH by 10-fold ($p < 0.05$). Biodistribution data exhibits peak tumor-specific uptake at 3h post-injection (3.1 a.u. pancreas, 0.003 a.u. liver, 0.002 a.u. kidney).

Conclusion: Increased signal values for the acidic pHs from NIR fluorescence and MSOT suggest that the V3-750 and V3FS-750 probes can each differentiate healthy cells from pancreatic cancer cells by targeting the acidic cell microenvironment.

Acknowledgements
The author wishes to thank R01CA2810908

Development of Perimidine based Squaraine Dyes for Optoacoustic Imaging

Shahir Sarasiyaa,b, William M. MacCuaigc, Lacey R. McNallyc,d, Maged Henary*a,b
a Department of Chemistry, Georgia State University, Atlanta, GA 30303, USA
b Center of Diagnostics and Therapeutics, Georgia State University, Atlanta, GA 30303, USA
c Stephenson Cancer Center, University of Oklahoma, Oklahoma City, OK 73104, USA
d Department of Surgery, University of Oklahoma, Oklahoma City, OK 73104, USA
* mhenary1@gsu.edu

Abstract

Optoacoustic imaging is an emerging bioimaging technique that combines optical excitation and ultrasound detection to generate a signal. The signal is generated through the optoacoustic effect, and the signal generated can be tracked at multiple wavelengths by Multispectral optoacoustic tomography (MSOT). As sound waves are the detection method, they have lower light scattering in tissue compared to light, allowing for deeper tissue penetration and higher-resolution images. For optoacoustic imaging contrast agents, the two main criteria are optimal: strong absorbance and weak fluorescence. Current agents are designed for fluorescence imaging, resulting in poor signal intensity and spectral shape, making them not applicable for optoacoustic imaging. Squaraine dyes are a class of Near Infrared (NIR) region scaffolds that have shown promising biological applications. The drive to achieve NIR region optical properties is due to biomolecules having limited to no interference in this region. This allows for deeper penetration into the cell and a better signal-to-noise ratio.

Current squaraine dyes primarily utilize the indolium heterocycles, which are designed for fluorescence imaging in the NIR region. In addition, indolium-based squaraine dye has an absorbance below 700 nm, which underutilizes the full NIR potential. When the perimidine heterocycle is introduced to squaraine dyes, the absorbance is redshifted to over 800 nm. Perimidine-based squaraine is designed to be an optoacoustic imaging contrast agent due to strong absorbance and weak fluorescence. Herein, we report the synthesis, optical properties, and initial optoacoustic imaging data for the new squaraine dyes. These perimidine-based squaraine dyes have shown high optoacoustic signal and unique spectral shape that range the NIR region

STUDENT

Examining the Relationship Between Adverse Childhood Experience Scores and Quality of Life Scores in Patients Undergoing Radiotherapy for Head and Neck Cancer

Katherine Swenson1*, Meng-Lun Hsieh2 , Daniel Zhao3 , Christina Henson4
1The University of Oklahoma College of Medicine
2UT Southwestern Department of Radiation Oncology
3Department of Biostatistics and Epidemiology, OUHSC
4The University of Oklahoma College of Medicine Department of Radiation Oncology
* katherine-swenson@ouhsc.edu

Purpose: Adverse childhood experiences (ACEs) have been linked to a multitude of diseases, including cancer. ACEs are potentially traumatic events that occur before 18 years of age and can include, but are not limited to: abuse, neglect, exposure to violence, or having a caregiver who struggles with mental health or substance abuse. While previous, long-standing studies have found an association between elevated ACE scores and cancer risk

[1], little is known about the relationship between ACE scores and quality of life changes throughout cancer treatment. Elevated ACE scores have been linked to altered stress responses in adults, and because of this, we hypothesize that patients with higher ACE scores will have a greater decrease in their quality-of-life scores while undergoing radiotherapy for head and neck cancer.

Methodology: This study was conducted on a prospective protocol with IRB approval. Patients with head and neck cancer completed a ten question ACE survey during their clinic visit, prior to beginning radiotherapy. Patients also completed the EORTC Core Quality of Life questionnaire that measures their psycho-social, physical, and social well-being prior to beginning treatment, and then again at the end of treatment, roughly six weeks later. Spearman correlation coefficients and the t-test were used to calculate relationships.

Results: Interim data from 14 patients undergoing treatment for head and neck cancer has been collected. Spearman correlation coefficient test found a moderate relationship between emotional function decline throughout treatment in patients who reported the adverse childhood experience of living with a mentally ill caregiver. Furthermore, patients who reported feeling unloved by their family throughout childhood reported higher rates of physical pain (p-value = 0.019).

Conclusion: This study aims to gather quality of life data from 100 patients. Preliminary data has shown an association between certain ACEs and a decline in emotional functioning as well as increased reported pain that has affected patients' quality of life. Patients with increased numbers of ACEs likely have more trauma, and previous studies have found decreased resiliency and coping ability in patients with traumatic childhoods. Unfortunately, trauma-informed care is still underutilized in medicine. We hope that by understanding the roles that ACEs can have on quality of life throughout and after cancer treatment, we can strategize ways to improve patient experiences and outcomes.

References

1. Felitti, V.J., et al., Relationship of childhood abuse and household dysfunction to many of the leading causes of death in adults. The Adverse Childhood Experiences (ACE) Study. Am J Prev Med, 1998. 14(4): p. 245-58.

STUDENT

Fluorescent Monitoring of Omeprazole-Mediated Autophagy in Pancreatic Adenocarcinoma

Karl N. Thomas1, Rohit Singh2, Lacey McNally2
1University of Oklahoma Health Sciences Department of Pharmaceutical Sciences
2University of Oklahoma Health Sciences Department of Surgery

Background: Pancreatic adenocarcinoma (PADC) is associated with poor clinical outcomes that show resistance to apoptosis. Therefore, we explored an off-label use of Omeprazole to discover its effect on PADC. Neutral Red (NR) and Acridine Orange (AO) are useful probes to detect autophagy due to their characteristic emission shift when protonated by acidic cellular bodies. Our goal was to expose underlying cellular processes which are differentially regulated by Omeprazole to aid in treatment design and improve patient outcomes.

Methods: Freshly cultured S2VP10, Suit2, and Panc1 cells were treated with 50uM Omeprazole for 4 hours before fluorescent NR dye staining to assess cell viability. Pancreatic cancer cells were treated with Omeprazole for 4, 7, and 24h followed by treatment with 10uM Acridine Orange to assess changes in lysosome activity. Finally, the activity of ion channels ASIC1 and ASIC3 was measured using immunofluorescence on Omeprazole-treated S2VP10 and Suit2 pancreatic cancer cells, immunofluorescence. Fluorescent staining was analyzed using Nikon NIS Elements. Fluorescence intensity within relevant regions were normalized to region area. Significance was determined using Kruskal-Wallis tests followed by pairwise Wilcoxon pos hoc tests. Differences were considered statistically significant at $p<0.05$

Results: Following Omeprazole treatment, mean NR fluorescence decreased by 25.0%, 13.1%, and 31.4% respectively for S2VP10, Suit2, and Panc1 cells indicating decreased lysosomal activity or membrane integrity. AO staining qualitative analysis of morphology retention and punctate zones of red fluorescence in the cytoplasm indicates that cells are undergoing autophagy (Figure 1). Additionally, autophagy is increased for treatment groups with maximum apparent autophagy occurring after 4-hours of treatment. Significantly increased ASIC1 and ASIC3 staining was observed for the 4-hour treatment groups compared to controls in both S2VP10 and Suit2 cells lines.

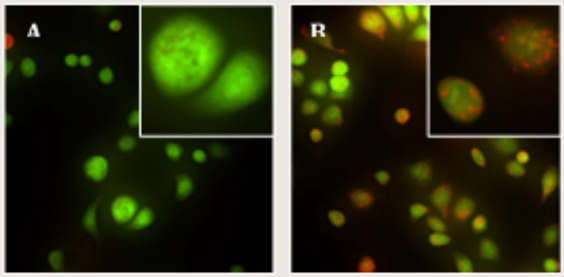

Figure 1. Acridine Orange stain of S2VP10 cells for (A) untreated controls and (B) 7-hour 50uM Omeprazole treated S2VP10 cells.

Discussion: Omeprazole is a proton pump inhibitor, and our results show it has a significant effect on the proton compartmentalization within pancreatic cancer. Treatment of PDAC remains challenging due to its enhanced autophagy expression which enables cell survival despite nutrient deprivation. We have shown that use of proton inhibitors like Omeprazole disrupts the autophagy mechanism. Exploiting this effect may help to reduce chemoresistance in PDAC.

Acknowledgements: NIH: R01CA281098

Assessment of phenylalanine modified pH low insertion peptide for identification of pancreatic cancer.

Sylvana Knapp1, Ryan C. Bynum2, Happy Agarwal2, Lacey R. McNally2
1Oklahoma School of Science and Mathematics High School
2University of Oklahoma Health Science Center
* sylvana.knapp@ossm.edu

Introduction

Pancreatic cancer is very aggressive and has only a 12.8% relative survival rate, which is why it is vital to remove the entirety of the cancer during surgery. Although only 20% of patients are eligible for surgical treatment, the majority of these patients will have positive margins. To overcome this limitation, we investigate the potential of developing a peptide-targeted contrast agent (V7Phe) to identify acidic pH using near-infrared fluorescence imaging (NIR) and multispectral optoacoustic imaging (MSOT) to improve cancer detection.

Method

We synthesized V7 and V7Phe pH low using microwave chemistry, removal of resin, lyophilization, and rehydration. The peptides were conjugated to HiLyte 750 dye using maleimide chemistry, dialyzed, and conjugation of the peptide to the dye was confirmed via spectroscopy. S2VP10 pancreatic cancer cell line was plated and acclimated to 7.4 pH and 6.6 pH media to mimic a healthy microenvironment and an acidic tumor microenvironment. Near-Infared fluorescence imaging was used to measure the probe uptake.

Results

In S2VP10 cells, the V7Phe probe has higher signal at pH 7.4 (control) and pH 6.6 (tumor) when compared to V7 ($p<0.01$). V7Phe has greater signal at pH 6.6 vs V7Phe at pH 7.4 ($p<0.01$). V7Phe had improved solubility vs V7 in that it was soluble in wáter as opposed to V7 which often requires DMF.

Conclusion

The greater signal at pH 6.6 suggests that the V7Phe probe may contrast acidic cancer cells from healthy cells by targeting the acidic cancer microenvironment. Phenylalanine is not necessarily the best peptide for signaling, but it was the best for solubility.

The Impact of Gliomas on the Normal Brain Microenvironment: A Pilot Study

Nicole L. Riha, Jacen S. Moore, Sheila Criswell
College of Health Professions, University of Tennessee Health Science Center, 930 Madison Ave., Memphis, TN

Gliomas are malignant tumors of neuronal support cells within the central nervous system (CNS) and are characterized by poor overall prognoses and limited treatment options due to their infiltrative growth patterns. The neural tumor microenvironment, composed of benign neurons, neuroglia, endothelial cells, and intravascular white blood cells, is a target-rich site for potential chemotherapeutic agents. This study assessed cell proliferation rates, white blood cell components, and a limited number of nuclear, cytoplasmic, and membrane markers using immunohistochemistry (IHC) assays on formalin-fixed and paraffin-embedded benign and glial tumor tissue samples from the CNS. It was observed that glioma tissues had increased rates of glial cell proliferation, and significant increases in the number of observed T-lymphocytes and granulocytes, but decreased expression of markers SSTR2, L1CAM, and GATA3 when compared to benign tissue samples. A more detailed characterization of the migratory and population expansion potential of the gliomal microenvironment could provide valuable therapeutic target combinations for use in the development of future treatments.

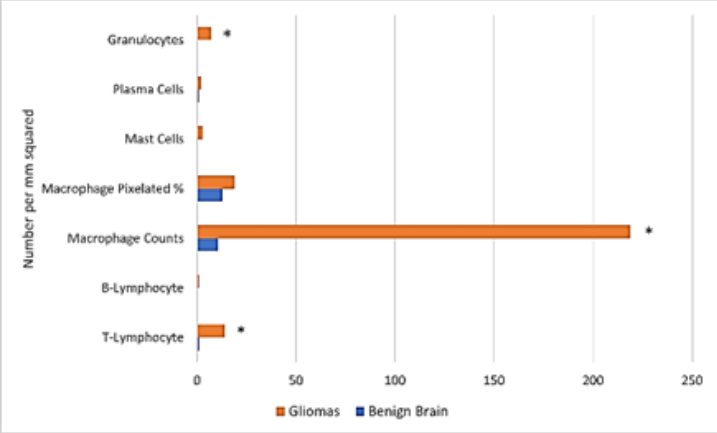

Figure 1. Figure 3. Immunohistochemistry labeling results for white blood cell populations between gliomas and normal brain tissues. Granulocytes and T-lymphocytes were found to be statistically increased in glioma tissues. Although macrophages were noted to be increased in gliomas in both methods of enumeration, they did not reach statistical significance for the automated method to determine percent labeling in tissues.

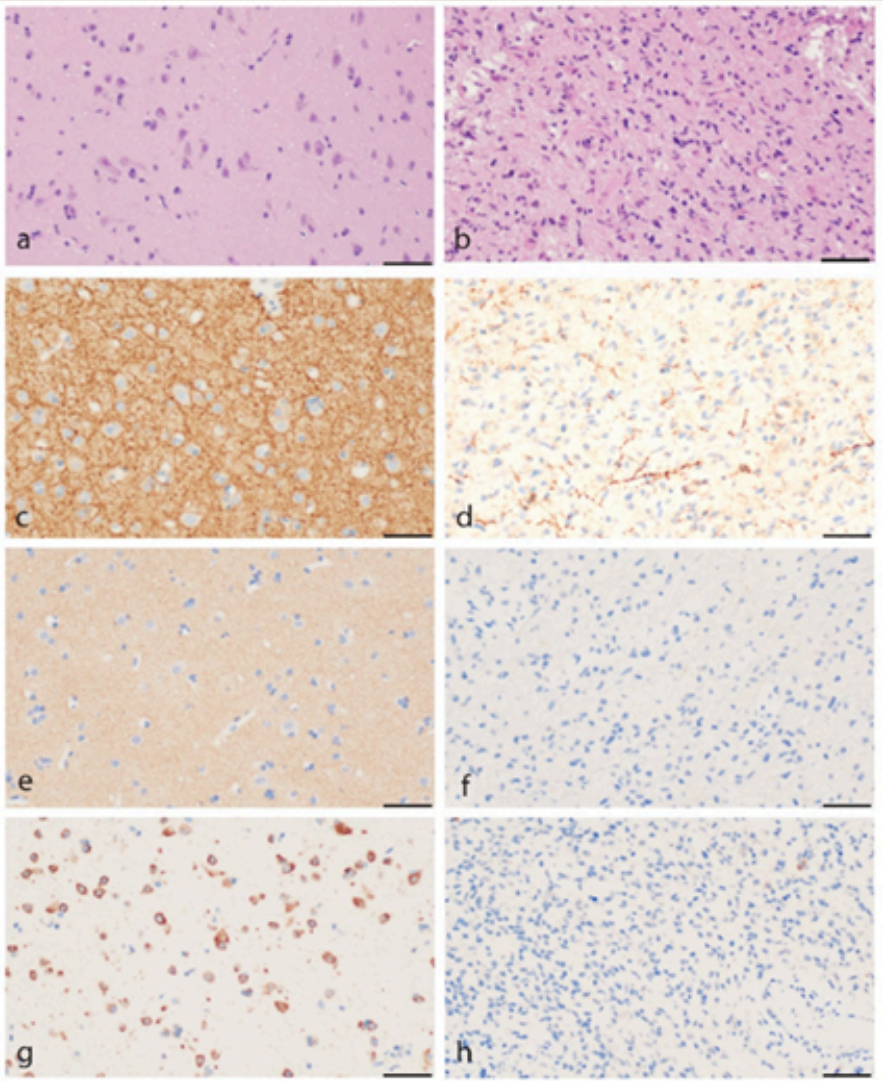

Figure 2. Benign CNS and glioma tissues with H&E and labeled with diaminobenzidine immunohistochemistry. (a) Benign and (b) malignant CNS stained with H&E. (c) Positive labeling (brown chromogen) of SSTR2 in benign brain tissues as compared with (d) glioma which evidenced a lower receptor expression. (e) Increased L1CAM expression in benign tissue as compared with (f) gliomas. (g) Higher GATA3 transcription factor expression in benign tissues as compared with (h) gliomas. Scale bar = 50 μm. Images were taken with 40x objective.

Histological Methods for Plants

Sheila Criswell1, Brian Gaylord2, Christopher R. Pitzer3

1 Department of Diagnostic and Health Sciences, University of Tennessee Health Science Center, Memphis, TN, USA
2 UT DermPath, a division of University Clinical Health, University of Tennessee Health Science Center, Memphis, TN, USA
3 Department of Physiology, College of Graduate Health Sciences, University of Tennessee Health Science Center, Memphis, TN, USA

The authors explored the histological challenges of working with plant tissues by collecting various flora representing the four main plant organs: leaf, stem, root, and flower/fruit. Triplicate samples of each specimen were placed in formalin for paraffin embedding, in formalin for later frozen sections, and used fresh for immediate frozen sectioning. Frozen sections of plant tissues were more challenging to obtain than formalin-fixed paraffin-embedded (FFPE) sections, showed tissue loss during staining, and were morphologically inferior to FFPE sections. Historically, plant tissue fixation and processing have used different reagents compared to animal tissue processing and required significantly longer times. However, this investigation found that reagents and protocols from a modern histology laboratory processing mammalian tissues can be applied to plant tissue processing with only slight modifications in reagent timing. Additionally, while it is well-known that plant cell walls stain well with safranin O, this study found that the uptake of safranin O can be accelerated by incubating at 60°C.

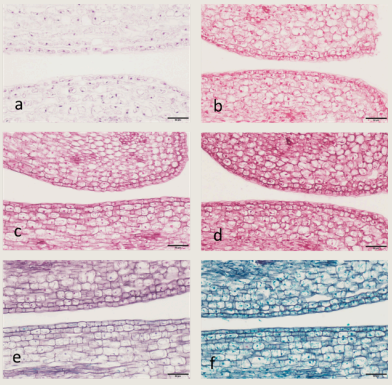

Figure 1. Formalin-fixed paraffin-embedded sections of broccoli stained with (a) H&E which shows good nuclear staining, but poor cytoplasmic staining. However, tissues stained with Safranin O for (b) 1 hour at room temperature demonstrates improved cytoplasmic staining. Safranin O stain at (c) room temperature for 24 hours or at (d) 60°C for 1 hour show similar improved staining over (b). The fast green counterstain (e,f) applied for 1 minute after safranin O appeared less vibrant when dehydrated through alcohols (e) when compared to the air-dried method of dehydration (f). Scale bar = 50 µm.

STUDENT

Nada-Saleh poster

Title: Temporally Multiplexed Imaging of Cell Cycle Dynamics Using Reversibly Photoswitchable Fluorescent Proteins in FUCCI4 Cells

Cilia are evolutionary conserved organelles that extend from the centriole. The cilium cycles assembly and disassembly depending on the cell-cycle; the formation of the cilium typically occurs during G0/G1 phase of the cell cycle, whereas the cilium is disassembled prior to mitosis, as centrioles participate in spindle formation. Our research focuses on imaging the entire process of the cilium formation to understand how ciliary/centriolar proteins orchestrate to form the cilium in coordination with the cell cycle. To visualize the complexed protein dynamics, we seek to establish a method that allows us to simultaneously image a dozen of ciliary/centriolar proteins using the recently developped Temporally Multiplexed Imaging (TMI) technique (PMID: 38029746). This novel approach utilizes reversibly photoswitchable fluorescent proteins (rsFPs) with distinct off-switching rates. The combined spectrally similar signal with different photoswitching kinetics can be unmixed into a linear combination of the kinetics from each fluorophore, which allows concurrent visualization of more than four fluorophores, a typical limit of the standard microscope. To prove the concept of TMI using Fluorescent Ubiquitination-based Cell Cycle Indicator 4 (Fucci4), I generated cell lines stably expressing four cell cycle markers (Cdt1, Geminin, SLBP, and Histon H1), each of which is tagged with a different photoswitchable protein with similar excitation/emission spectra. I then performed live-cell imaging and analyzed the data using MATLAB-based linear algebra techniques and least squares regression for unmixing. In this presentation, I will show the data from my recent experiments, and discuss challenges toward successful visualization of ciliogenesis process using the TMI technologies.

STUDENT

Assessment of V3 variants to identify pancreatic cancer

Emma Sanderson1, Ryan Bynum2, Tereza Husarova3, Lacey McNally4
1 Department of Chemistry, University of Oklahoma
2 Department of Surgery, University of Oklahoma Health Science Center
3 Department of Surgery, Military Hospital Prague, Czech Republic
4 Department of Surgery, University of Oklahoma Health Science Center

Background: Pancreatic ductal adenocarcinoma (PDAC) is generally detected late and patients have poor outcomes. Current methods to identify pancreatic cancer generally involve 3D imaging techniques such as CT. However, CT has inferior resolution and often is unable to differentiate live pancreatic tumors from fibrosis. To overcome these limitations, we employed optoacoustic imaging combined with the pH-sensitive peptide probe, V3, to identify pancreatic cancer in orthotopic mouse models.

Methods: We utilized microwave chemistry to synthesize the V3 peptide or V3FS, resulting in a purity of greater than 90%. The V3 or V3FS peptide was then conjugated to a fluorescent dye and dialyzed to make the V3-750 or V3FS-750 probe. S2VP10 and S2013 pancreatic cancer cell lines were plated in 6-well plates and acclimated to 7.4, 6.8, and 6.6 to mimic the healthy cell microenvironment and the pancreatic cancer cell microenvironment. Cells were treated with 1 micromolar of the V3-750 or V3FS-750 probe for 1 hour, then imaged with the near-infrared (NIR) fluorescence imager. Cells were then scraped and loaded into tissue mimicking phantoms and imaged with multispectral optoacoustic tomography (MSOT). Athymic mice were orthotopically injected with S2VP10 cells and tumors grew to 3 mm. The V3-750 or V3FS-750 probes were intravenously injected, and mice were imaged 3h post-injection with MSOT.

Results: NIR fluorescence signal values for the samples displayed a trend that the V3-750 and V3FS-750 probes targeted 6.6 and 6.8 pH environments more than the 7.4 pH environment. MSOT data supported this trend, with the signal values from 6.6 and 6.8 pH being greater than the 7.4 pH by 10-fold ($p < 0.05$). Biodistribution data exhibits peak tumor-specific uptake at 3h post-injection (3.1 a.u. pancreas, 0.003 a.u. liver, 0.002 a.u. kidney).

Conclusion: Increased signal values for the acidic pHs from NIR fluorescence and MSOT suggest that the V3-750 and V3FS-750 probes can each differentiate healthy cells from pancreatic cancer cells by targeting the acidic cell microenvironment.

Acknowledgements
The author wishes to thank R01CA2810908

https://biologicalstaincommission.org/

Nada Saleh

Affiliation: Oklahoma University Health Sciences Center

Email: nada-saleh@ouhsc.edu

Title: Temporally Multiplexed Imaging of Cell Cycle Dynamics Using Reversibly Photoswitchable Fluorescent Proteins in FUCCI4 Cells

Abstract

Cilia are evolutionary conserved organelles that extend from the centriole. The cilium cycles assembly and disassembly depending on the cell-cycle; the formation of the cilium typically occurs during G0/G1 phase of the cell cycle, whereas the cilium is disassembled prior to mitosis, as centrioles participate in spindle formation. Our research focuses on imaging the entire process of the cilium formation to understand how ciliary/centriolar proteins orchestrate to form the cilium in coordination with the cell cycle. To visualize the complexed protein dynamics, we seek to establish a method that allows us to simultaneously image a dozen of ciliary/centriolar proteins using the recently developped Temporally Multiplexed Imaging (TMI) technique (PMID: 38029746). This novel approach utilizes reversibly photoswitchable fluorescent proteins (rsFPs) with distinct off-switching rates. The combined spectrally similar signal with different photoswitching kinetics can be unmixed into a linear combination of the kinetics from each fluorophore, which allows concurrent visualization of more than four fluorophores, a typical limit of the standard microscope. To prove the concept of TMI using Fluorescent Ubiquitination-based Cell Cycle Indicator 4 (Fucci4), I generated cell lines stably expressing four cell cycle markers (Cdt1, Geminin, SLBP, and Histon H1), each of which is tagged with a different photoswitchable protein with similar excitation/emission spectra. I then performed live-cell imaging and analyzed the data using MATLAB-based linear algebra techniques and least squares regression for unmixing. In this presentation, I will show the data from my recent experiments, and discuss challenges toward successful visualization of ciliogenesis process using the TMI technologies.

Samrita Dogra[1,2*] and Bethany N. Hannafon[1,2]

Affiliations: [1]Department of Obstetrics and Gynaecology and [2]Peggy and Charles Stephenson Cancer Center, The University of Oklahoma Health Sciences Center, Oklahoma City, Oklahoma, USA.

***Email**: samrita-dogra@ouhsc.edu

Abstract

Peritoneal metastasis is one of the leading causes of mortality in high-grade serous ovarian cancer (HGSOC) which results in a dismal 5-year survival rate of 17–39%. To establish peritoneal metastasis, disseminated tumor cells as clusters/ spheroids (1) adhere to the organs in the peritoneal cavity, (2) breach the barrier of mesothelial cell monolayer and (3) invade into the underlying extracellular matrix network. Therefore, to develop effective therapeutics for treating peritoneal metastasis it is imperative to have model systems that can help study the crosstalk between ovarian cancer cell spheroids and mesothelial cells *in vitro*. Our protocol is adapted from previously described methods that are based on fluorescent microscopy. Our approach takes advantage of the Incucyte live cell imaging system to monitor the interaction between tumor cells and mesothelial cells in real time using cell tracking dyes and is amenable for high throughput screening. The ovarian cancer cells were stained with the CellTracker green CMFDA dye and allowed to form spheroids while the mesothelial cells were stained with the CellTracker Red CMPTX dye. Our data shows that the ovarian cancer spheroids induced migration of the mesothelial cells away from the spheroids resulting in formation of a hole. The area of hole/ negative space can be quantified over time to compare the differences in both the rate and extent of clearance between control and experimental ovarian cancer cells. Additionally, we have used this protocol to evaluate the efficacy of different drugs to inhibit early steps of ovarian cancer metastasis. As this assay requires fewer cells and/ or spheroids and use of cell tracker dyes, primary mesothelial cells and spheroids-derived from ovarian cancer patient ascites can be used to evaluate efficacy of drugs that could potentially inhibit metastasis.

Acknowledgements

The author wishes to thank the Office of the Assistant Secretary of Defense for Health Affairs (Ovarian Cancer Research Program) for the funding support (Award No.: HT9425-23-1-0223).